TECHNISCHE UNIVERSITÄT
KAISERSLAUTERN

Variational Methods for Manifold-valued Image Processing

Ronny Bergmann[a]
University of Kaiserslautern

Seminars in Mathematical Engineering, ICTEAM,
Université catholique de Louvain,

Louvain-la-Neuve, March 21, 2017

[a] joint work with M. Bačák (MPI MIS Leipzig), J. Persch, G. Steidl (U Kaiserslautern), D. Tenbrinck (WWU Münster), A. Weinmann (H Darmstadt)

Contents

Introduction

Manifold-valued images

New data aquisition modalities $\Rightarrow$ non-Euclidean range of data

- **Interferrometric synthetic aperture radar (InSAR)**
- Surface normals
- Diffusion tensors in magnetic resonance imaging (DT-MRI)
- Electron backscattered diffraction (EBSD)
- Directional data: wind, flow, GPS,...

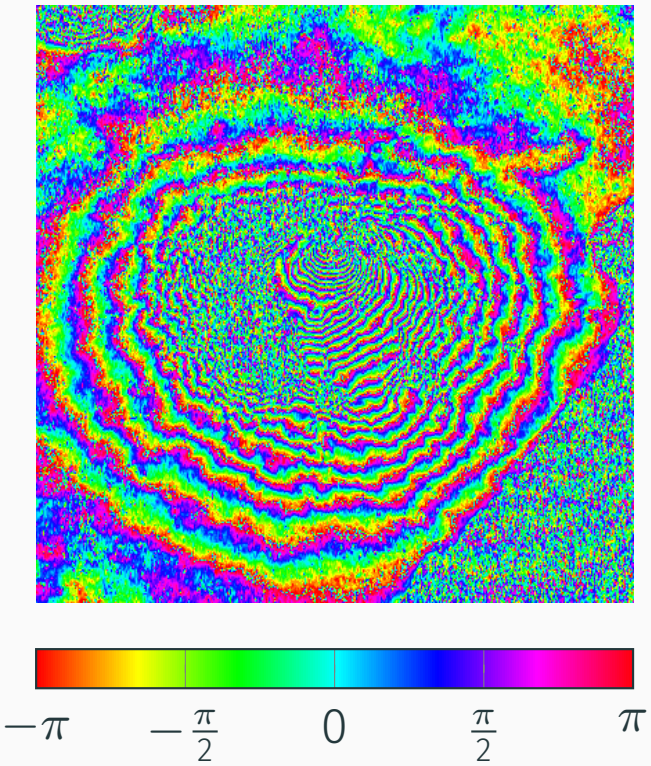

InSAR data of Mt. Vesuvius
[Rocca, Prati, Guarnieri 1997]

Manifold-valued images

New data aquisition modalities $\Rightarrow$ non-Euclidean range of data

- Interferrometric synthetic aperture radar (InSAR)
- **Surface normals**
- Diffusion tensors in magnetic resonance imaging (DT-MRI)
- Electron backscattered diffraction (EBSD)
- Directional data: wind, flow, GPS,...

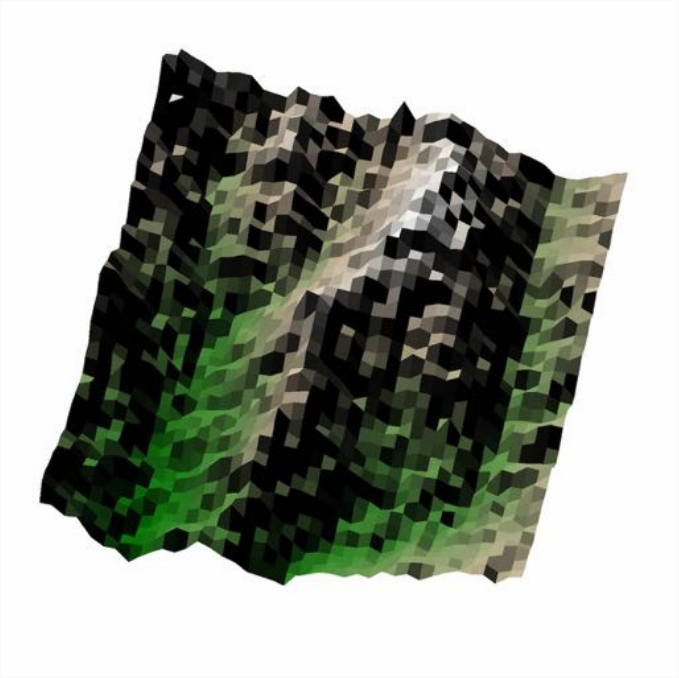

National elevation dataset
[Gesch, Evans, Mauck, 2009]

Manifold-valued images

New data aquisition modalities $\Rightarrow$ non-Euclidean range of data

- Interferrometric synthetic aperture radar (InSAR)
- Surface normals
- **Diffusion tensors in magnetic resonance imaging (DT-MRI)**
- Electron backscattered diffraction (EBSD)
- Directional data: wind, flow, GPS,...

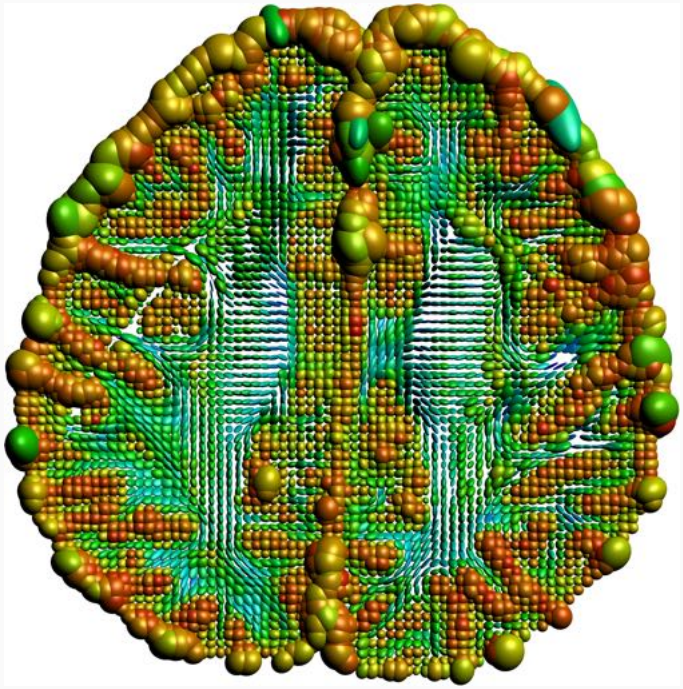

Slice # 28 from the Camino data set
http://cmic.cs.ucl.ac.uk/camino

Manifold-valued images

New data aquisition modalities $\Rightarrow$ non-Euclidean range of data

- Interferrometric synthetic aperture radar (InSAR)
- Surface normals
- Diffusion tensors in magnetic resonance imaging (DT-MRI)
- **Electron backscattered diffraction (EBSD)**
- Directional data: wind, flow, GPS,...

EBSD example from the MTEX toolbox
[Bachmann, Hielscher, since 2005]

A first example: phase valued data

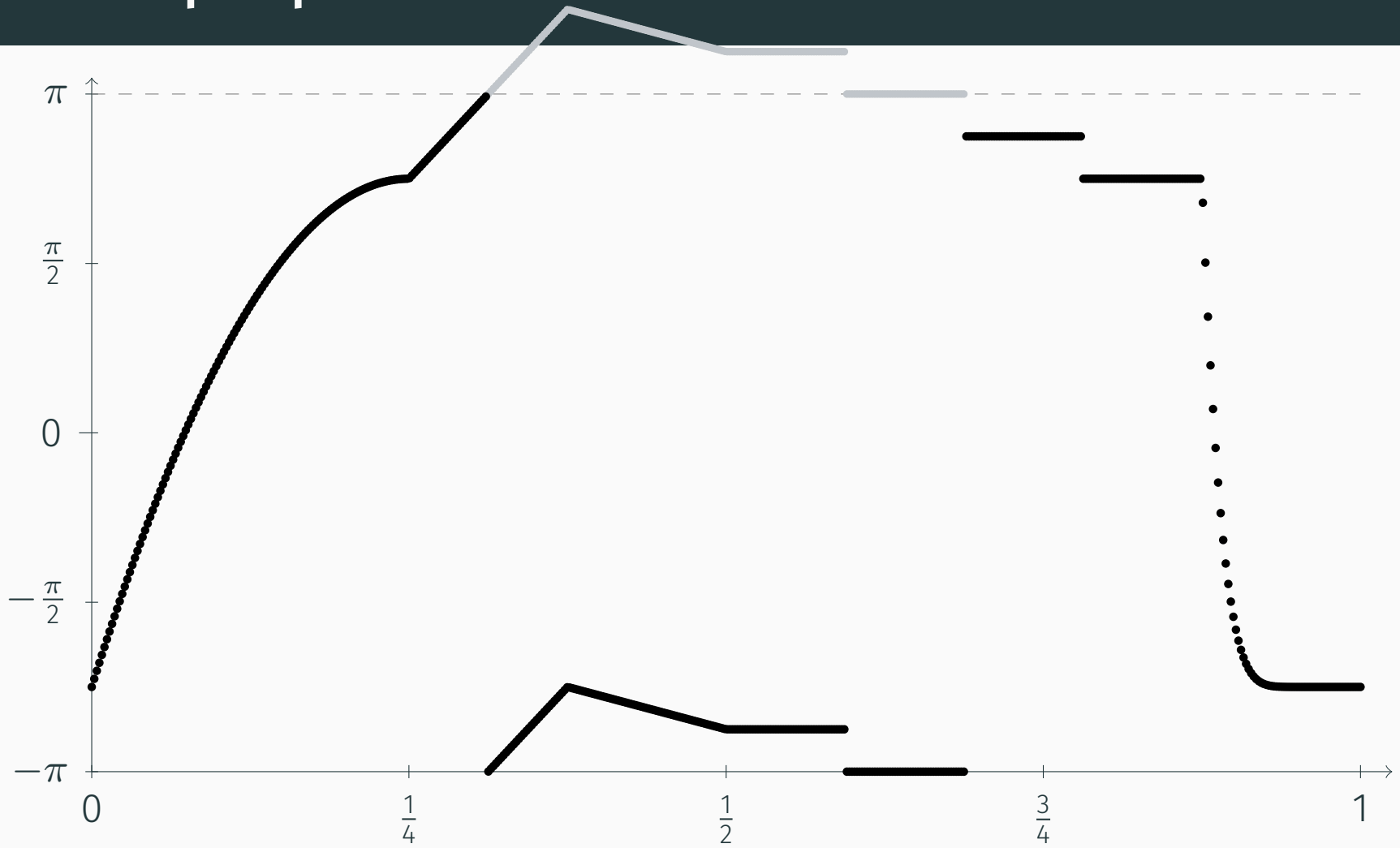

- function $f\colon [0,1] \to \mathbb{S}^1$ sampled to obtain data $f_{\mathrm{o}} = (f_{\mathrm{o},i})_{i=1}^{500}$
- f could be a wrapped version of the gray plot, hence
- jumps $> \pi$ at $\frac{5}{16}$ and $\frac{11}{16}$ are due to the representation system

A first example: phase valued data

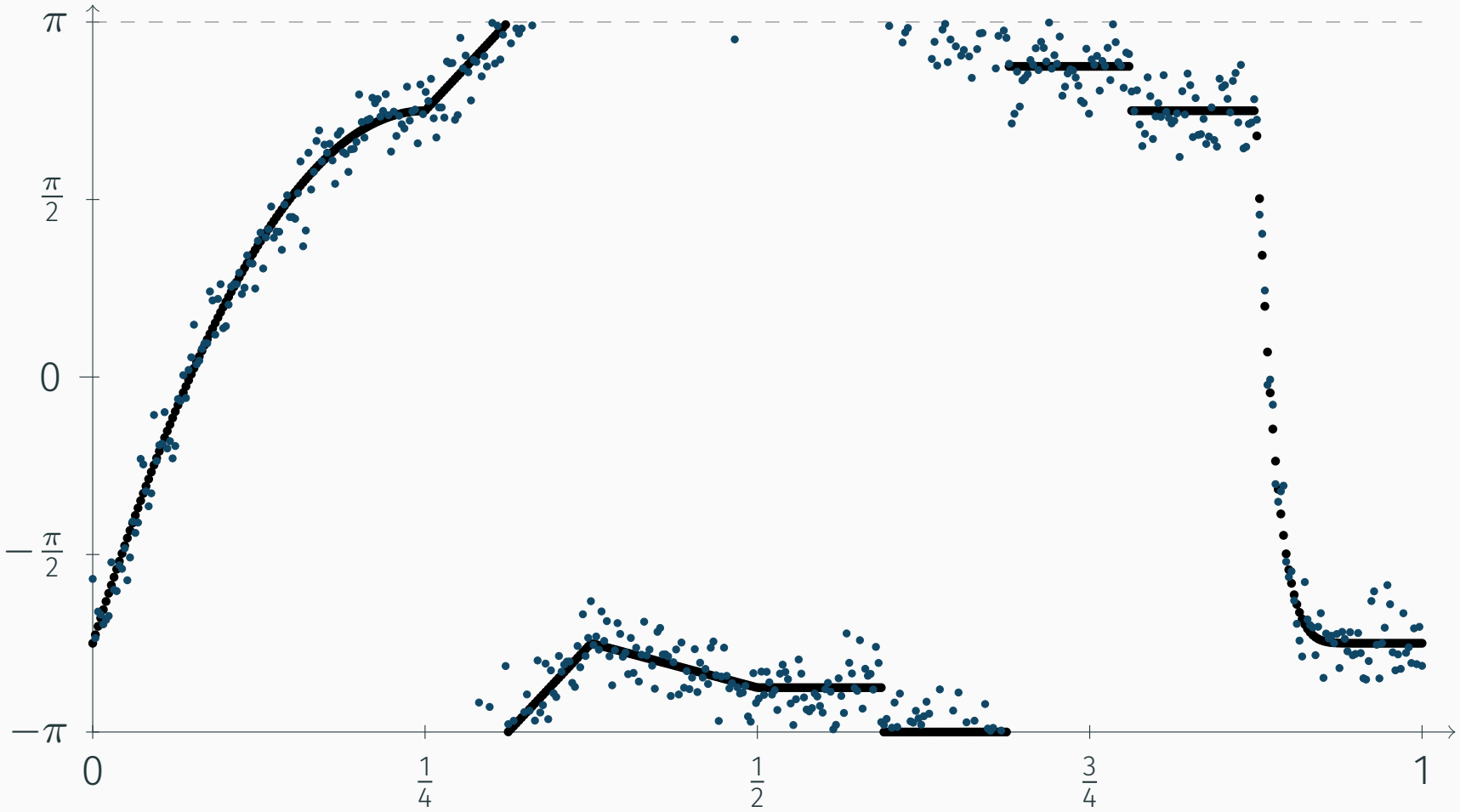

- function $f\colon [0,1] \to \mathbb{S}^1$ sampled to obtain data $f_{\mathrm{o}} = (f_{\mathrm{o},i})_{i=1}^{500}$
- adding wrapped Gaussian noise, $\sigma = 0.2$
- noisy data $f_{\mathrm{n}} = (f_{\mathrm{o}} + \eta)_{2\pi}$

Tasks in image processing

In image processing of gray- or color-valued images, usual tasks are

- denoising
- inpainting
- combined inpainting & denoising
- feature extraction
  - edge detection
  - texture classification
  - labeling/clustering
- deblurring

Variational models for real valued data

- given noisy image $f : \mathcal{V} \to \mathbb{R}$, $\mathcal{V} \subseteq \mathcal{G} = \{1, \dots, N\} \times \{1, \dots, M\}$
- **reconstruct** original image $u_0 : \mathcal{G} \to \mathbb{R}$, inpaint pixel from $\mathcal{G} \backslash \mathcal{V}$
- approach: find minimizer u^* of a **variational model**

$$\mathcal{E}(u) := \underbrace{\mathcal{D}(u; f)}_{\text{data term}} + \underbrace{\alpha\, \mathcal{R}(u)}_{\text{regularization term}}, \qquad \alpha > 0.$$

- first order models (total variation, **TV**) [Rudin, Osher, Fatemi, 1992]
  - isotropic: $\mathcal{R}_{\text{iso}}(u) := \sum_{i,j} \left(|u_{i+1,j} - u_{i,j}|^2 + |u_{i,j+1} - u_{i,j}|^2 \right)^{\frac{1}{2}}$
  - anisotropic: $\mathcal{R}_{\text{aniso}}(u) := \sum_{i,j} \left(|u_{i+1,j} - u_{i,j}| + |u_{i,j+1} - u_{i,j}| \right)$
  - known to be edge preserving

Variational models for real valued data

- given noisy image $f : \mathcal{V} \to \mathbb{R}$, $\mathcal{V} \subseteq \mathcal{G} = \{1, \dots, N\} \times \{1, \dots, M\}$
- **reconstruct** original image $u_0 : \mathcal{G} \to \mathbb{R}$, inpaint pixel from $\mathcal{G} \backslash \mathcal{V}$
- approach: find minimizer u^* of a **variational model**

$$\mathcal{E}(u) := \underbrace{\mathcal{D}(u; f)}_{\text{data term}} + \underbrace{\alpha\, \mathcal{R}(u)}_{\text{regularization term}}, \qquad \alpha > 0.$$

- first order models (total variation, **TV**) [Rudin, Osher, Fatemi, 1992]
  - isotropic: $\mathcal{R}_{\text{iso}}(u) := \sum_{i,j} \left(|u_{i+1,j} - u_{i,j}|^2 + |u_{i,j+1} - u_{i,j}|^2 \right)^{\frac{1}{2}}$
  - anisotropic: $\mathcal{R}_{\text{aniso}}(u) := \sum_{i,j} \left(|u_{i+1,j} - u_{i,j}| + |u_{i,j+1} - u_{i,j}| \right)$
  - known to be edge preserving

Variational models for real valued data

- given noisy image $f : \mathcal{V} \to \mathbb{R}$, $\mathcal{V} \subseteq \mathcal{G} = \{1, \dots, N\} \times \{1, \dots, M\}$
- **reconstruct** original image $u_0 : \mathcal{G} \to \mathbb{R}$, inpaint pixel from $\mathcal{G} \backslash \mathcal{V}$
- approach: find minimizer u^* of a **variational model**

$$\mathcal{E}(u) := \underbrace{\mathcal{D}(u; f)}_{\text{data term}} + \underbrace{\alpha\, \mathcal{R}(u)}_{\text{regularization term}}, \qquad \alpha > 0.$$

- first order models (total variation, **TV**) [Rudin, Osher, Fatemi, 1992]
  - isotropic: $\mathcal{R}_{\text{iso}}(u) := \sum_{i,j} \left(|u_{i+1,j} - u_{i,j}|^2 + |u_{i,j+1} - u_{i,j}|^2 \right)^{\frac{1}{2}}$
  - anisotropic: $\mathcal{R}_{\text{aniso}}(u) := \sum_{i,j} \left(|u_{i+1,j} - u_{i,j}| + |u_{i,j+1} - u_{i,j}| \right)$
  - known to be edge preserving

Variational models for real valued data

- given noisy image $f : \mathcal{V} \to \mathbb{R}$, $\mathcal{V} \subseteq \mathcal{G} = \{1, \dots, N\} \times \{1, \dots, M\}$
- **reconstruct** original image $u_0 : \mathcal{G} \to \mathbb{R}$, inpaint pixel from $\mathcal{G} \backslash \mathcal{V}$
- approach: find minimizer u^* of a **variational model**

$$\mathcal{E}(u) := \underbrace{\mathcal{D}(u; f)}_{\text{data term}} + \underbrace{\alpha\, \mathcal{R}(u)}_{\text{regularization term}}, \qquad \alpha > 0.$$

- first order models (total variation, **TV**) [Rudin, Osher, Fatemi, 1992]
  - isotropic: $\mathcal{R}_{\text{iso}}(u) := \sum_{i,j} \left(|u_{i+1,j} - u_{i,j}|^2 + |u_{i,j+1} - u_{i,j}|^2 \right)^{\frac{1}{2}}$
  - anisotropic: $\mathcal{R}_{\text{aniso}}(u) := \sum_{i,j} \left(|u_{i+1,j} - u_{i,j}| + |u_{i,j+1} - u_{i,j}| \right)$
  - known to be edge preserving
- higher order variational models avoid **stair casing effect**

[Chambolle, Lions, 1997; Setzer, Steidl, 2008; Bredies, Kunisch, Pock, 2010; Papafitsoros, Schönlieb, 2014]

Restoring images with values in Riemannian manifolds

Here:
Images with **pixel values** in a Riemannian manifold $\mathcal{M}$

Goal: **A Second Order Model for images** $f : \mathcal{V} \to \mathcal{M}$

Applications with manifold-valued images

$\mathbb{S}^1$	InSAR, HSI(HSV) color space, phase space
$\mathbb{S}^2$	directions, chromaticity-brightness color space
$\mathrm{SO}(3)$	orientations, electron backscattered diffraction
$\mathcal{P}(s)$	DT-MRI, covariance matrices

Notations on a Riemannian manifold $\mathcal{M}$

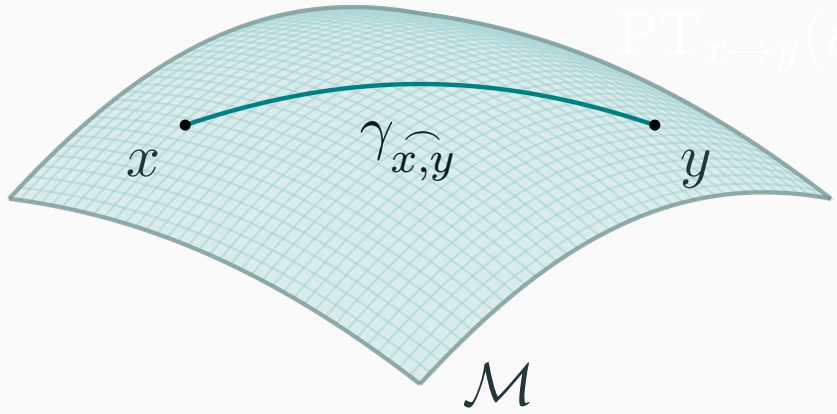

A d-dimensional manifold can be informally defined as a set $\mathcal{M}$ covered with a "suitable" collection of charts, that identify subsets of $\mathcal{M}$ with open subsets of $\mathbb{R}^d$.

[Absil, Mahony, Sepulchre, 2008]

Notations on a Riemannian manifold $\mathcal{M}$

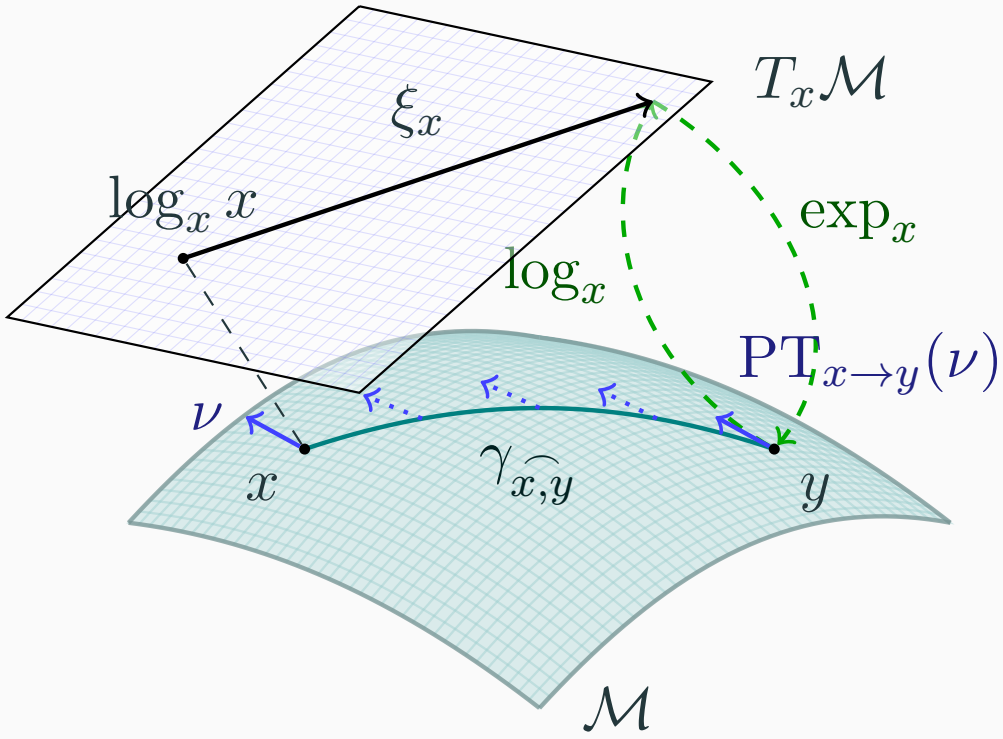

geodesic $\gamma_{\widehat{x,y}}$ shortest path (on $\mathcal{M}$) connecting $x, y \in \mathcal{M}$.
tangential plane $\mathrm{T}_x\mathcal{M}$ at x, $\mathrm{T}\mathcal{M} := \cup_{x\in\mathcal{M}} \mathrm{T}_x\mathcal{M}$
logarithmic map $\log_x y = \dot{\gamma}_{\widehat{x,y}}(0)$, "velocity towards y"
exponential map $\exp_x \xi_x = \gamma(1)$, where $\gamma(0) = x$, $\dot{\gamma}(0) = \xi_x$
parallel transport $\mathrm{PT}_{x\to y}(\nu)$ of $\nu \in \mathrm{T}_x\mathcal{M}$ along $\gamma_{\widehat{x,y}}$

Total variation regularization

First and second order differences

On $\mathbb{R}^n$

- line $\gamma(t) = x + t(y - x)$
- distance $\|x - y\|_2$
- first order model

$$\sum_{i \in \mathcal{V}} \|f_i - u_i\|_2^2 + \alpha \sum_{i \in \mathcal{G} \setminus \{N\}} \|u_i - u_{i+1}\|_2$$

Riemannian manifold $\mathcal{M}$

- geodesic path $\gamma_{\overset{\frown}{x,y}}(t)$
- geodesic distance $d\colon \mathcal{M} \times \mathcal{M} \to \mathbb{R}$
- first order model

[Strekalovskiy, Cremers, 2011; Lellmann et al., 2013; Weinmann et. al., 2014]

$$\sum_{i \in \mathcal{V}} d(f_i, u_i)^2 + \alpha \sum_{i \in \mathcal{G} \setminus \{N\}} d(u_i, u_{i+1})$$

First and second order differences

On $\mathbb{R}^n$

- line $\gamma(t) = x + t(y - x)$
- distance $\|x - y\|_2$
- first order model

$$\sum_{i \in \mathcal{V}} \|f_i - u_i\|_2^2 + \alpha \sum_{i \in \mathcal{G} \setminus \{N\}} \|u_i - u_{i+1}\|_2$$

- second oder difference

$$\|x - 2y + z\|_2$$

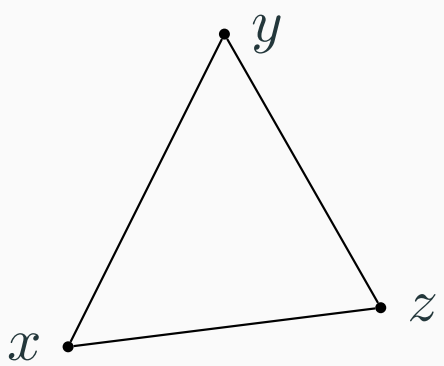

Riemannian manifold $\mathcal{M}$

- geodesic path $\gamma_{\widehat{x,y}}(t)$
- geodesic distance $d\colon \mathcal{M} \times \mathcal{M} \to \mathbb{R}$
- first order model

[Strekalovskiy, Cremers, 2011; Lellmann et al., 2013; Weinmann et. al., 2014]

$$\sum_{i \in \mathcal{V}} d(f_i, u_i)^2 + \alpha \sum_{i \in \mathcal{G} \setminus \{N\}} d(u_i, u_{i+1})$$

- How to model that on $\mathcal{M}$?

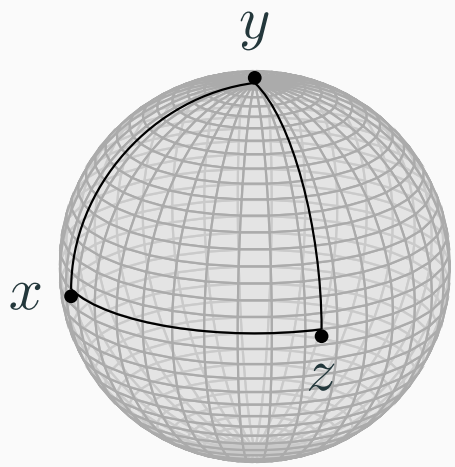

$\mathcal{M} = \mathbb{S}^2$

First and second order differences

On $\mathbb{R}^n$

- line $\gamma(t) = x + t(y - x)$
- distance $\|x - y\|_2$
- first order model

$$\sum_{i \in \mathcal{V}} \|f_i - u_i\|_2^2 + \alpha \sum_{i \in \mathcal{G} \setminus \{N\}} \|u_i - u_{i+1}\|_2$$

- second oder difference

$$2\|\tfrac{1}{2}(x + z) - y\|_2$$

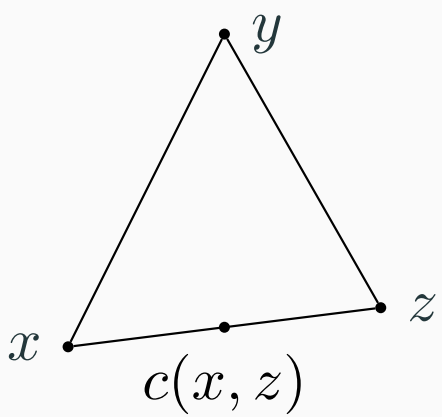

Riemannian manifold $\mathcal{M}$

- geodesic path $\gamma_{\widehat{x,y}}(t)$
- geodesic distance $d\colon \mathcal{M} \times \mathcal{M} \to \mathbb{R}$
- first order model

[Strekalovskiy, Cremers, 2011; Lellmann et al., 2013; Weinmann et. al., 2014]

$$\sum_{i \in \mathcal{V}} d(f_i, u_i)^2 + \alpha \sum_{i \in \mathcal{G} \setminus \{N\}} d(u_i, u_{i+1})$$

- **idea:** mid point formulation

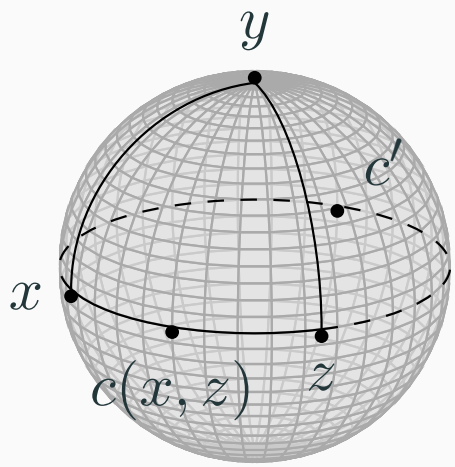

$\mathcal{M} = \mathbb{S}^2$

First and second order differences

On $\mathbb{R}^n$

- line $\gamma(t) = x + t(y - x)$
- distance $\|x - y\|_2$
- first order model

$$\sum_{i \in \mathcal{V}} \|f_i - u_i\|_2^2 + \alpha \sum_{i \in \mathcal{G} \setminus \{N\}} \|u_i - u_{i+1}\|_2$$

- second oder difference

$$2\|c(x, z) - y\|_2$$

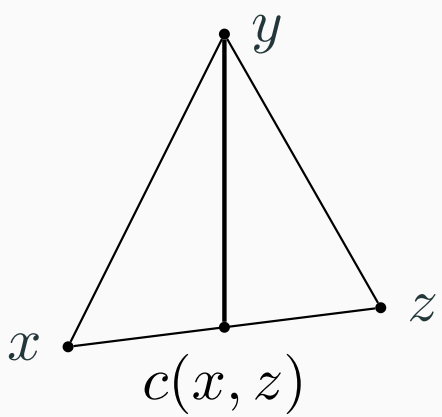

Riemannian manifold $\mathcal{M}$

- geodesic path $\gamma_{\widehat{x,y}}(t)$
- geodesic distance $d\colon \mathcal{M} \times \mathcal{M} \to \mathbb{R}$
- first order model

[Strekalovskiy, Cremers, 2011; Lellmann et al., 2013; Weinmann et. al., 2014]

$$\sum_{i \in \mathcal{V}} d(f_i, u_i)^2 + \alpha \sum_{i \in \mathcal{G} \setminus \{N\}} d(u_i, u_{i+1})$$

- **idea:** mid point formulation

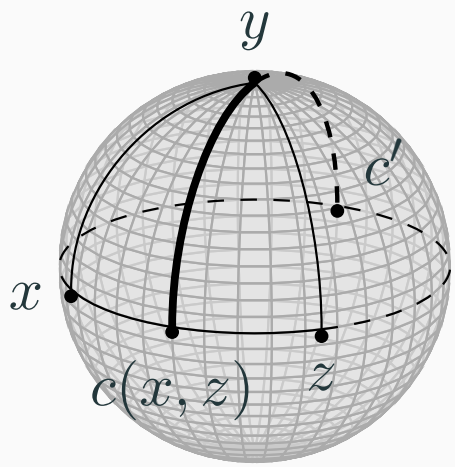

$\mathcal{M} = \mathbb{S}^2$

A second order TV-type model

Mid points between $x, z \in \mathcal{M}$:

$$\mathcal{C}_{x,z} := \left\{ c \in \mathcal{M} : c = \gamma_{\widehat{x,z}}\left(\tfrac{T}{2}\right) \text{ for any geodesic } \gamma_{\widehat{x,z}},\ T := \mathcal{L}(\gamma_{\widehat{x,z}}) \right\}$$

The **Absolute Second Order Difference**:

$$d_2(x,y,z) := \min_{c \in \mathcal{C}_{x,z}} d(c,y), \qquad x,y,z \in \mathcal{M}.$$

$\Rightarrow$ **Second Order TV-type Model** for $\mathcal{M}$-valued signals f

$$\mathcal{E}(u) := \sum_{i \in \mathcal{V}} d(f_i, u_i)^2 + \alpha \sum_{i \in \mathcal{G}\setminus\{N\}} d(u_i, u_{i+1}) + \beta \sum_{i \in \mathcal{G}\setminus\{1,N\}} d_2(u_{i-1}, u_i, u_{i+1})$$

For images additionally: use
$\|w - x + y - z\|_2 = 2\|\frac{1}{2}(w+y) - \frac{1}{2}(x+z)\|_2$ for
Absolute Second Order Mixed Difference

$$d_{1,1}(w,x,y,z) := \min_{c \in \mathcal{C}_{w,y}, \tilde{c} \in \mathcal{C}_{x,z}} d(c,\tilde{c}), \qquad w,x,y,z \in \mathcal{M}.$$

Proximal mappings and the CPP algorithm

To compute a minimizer of $\mathcal{E}(u)$: **proximal mappings**

For a function $\varphi\colon \mathcal{M}^n \to (-\infty, +\infty]$ and $\lambda > 0$ the **proximal mapping** is defined by [Moreau, 1965; Rockafellar, 1976; Ferreira, Oliveira, 2002]

$$\operatorname{prox}_{\lambda\varphi}(g) := \operatorname*{arg\,min}_{u \in \mathcal{M}^n} \frac{1}{2} \sum_{i=1}^{n} d(u_i, g_i)^2 + \lambda\varphi(u).$$

Note: For a minimizer u^* of φ it holds $\operatorname{prox}_{\lambda\varphi}(u^*) = u^*$.

Proximal mappings and the CPP algorithm

To compute a minimizer of $\mathcal{E}(u)$: **proximal mappings**

For a function $\varphi\colon \mathcal{M}^n \to (-\infty, +\infty]$ and $\lambda > 0$ the **proximal mapping** is defined by [Moreau, 1965; Rockafellar, 1976; Ferreira, Oliveira, 2002]

$$\operatorname{prox}_{\lambda\varphi}(g) := \operatorname*{arg\,min}_{u\in\mathcal{M}^n} \frac{1}{2}\sum_{i=1}^{n} d(u_i, g_i)^2 + \lambda\varphi(u).$$

Note: For a minimizer u^* of φ it holds $\operatorname{prox}_{\lambda\varphi}(u^*) = u^*$.

For $\varphi = \sum_{l=1}^{c} \varphi_l$ use **Cyclic Proximal Point Algorithm (CPPA)** [Bertsekas, 2011; Bačák, 2014]

$$x^{(k+\frac{l+1}{c})} = \operatorname{prox}_{\lambda_k\varphi_l}(x^{(k+\frac{l}{c})}), \quad i = 0, \dots, c-1,\ k > 0$$

For **real-valued data**: Converges to a minimizer if $\{\lambda_k\}_{k\in\mathbb{N}} \in \ell_2(\mathbb{Z})\backslash\ell_1(\mathbb{Z})$.

Minimizing the second order model

To minimize

$$\mathcal{E}(u) := \sum_{i\in\mathcal{V}} d(f_i, u_i)^2 + \alpha \sum_{i\in\mathcal{G}\setminus\{N\}} d(u_i, u_{i+1}) + \beta \sum_{i\in\mathcal{G}\setminus\{1,N\}} d_2(u_{i-1}, u_i, u_{i+1})$$

take each summand as one φ_l in the CPPA.
Parallelization: $c = 6$ (1D) or $c = 15$ (2D incl. mixed differences)

For the involved proximal maps we have

- $\varphi(u_i) = d(f_i, u_i)^2$: analytical solution [Ferreira, Oliveira, 2002]
- $\varphi(u_i, u_{i+1}) = d(u_i, u_{i+1})$: analytical solution [Weinmann, Storath, Demaret, 2014]
- $\varphi(u_{i-1}, u_i, u_{i+1}) = d_2(u_{i-1}, u_i, u_{i+1})$:
  - analytical solution for $\mathbb{S}^1$ [RB, Laus, Steidl, Weinmann, 2014]
  - numerical solution otherwise, using a gradient descent involving geodesic variation and Jacobi fields [Bačák, RB, Steidl, Weinmann, 2016]

A signal of cyclic data

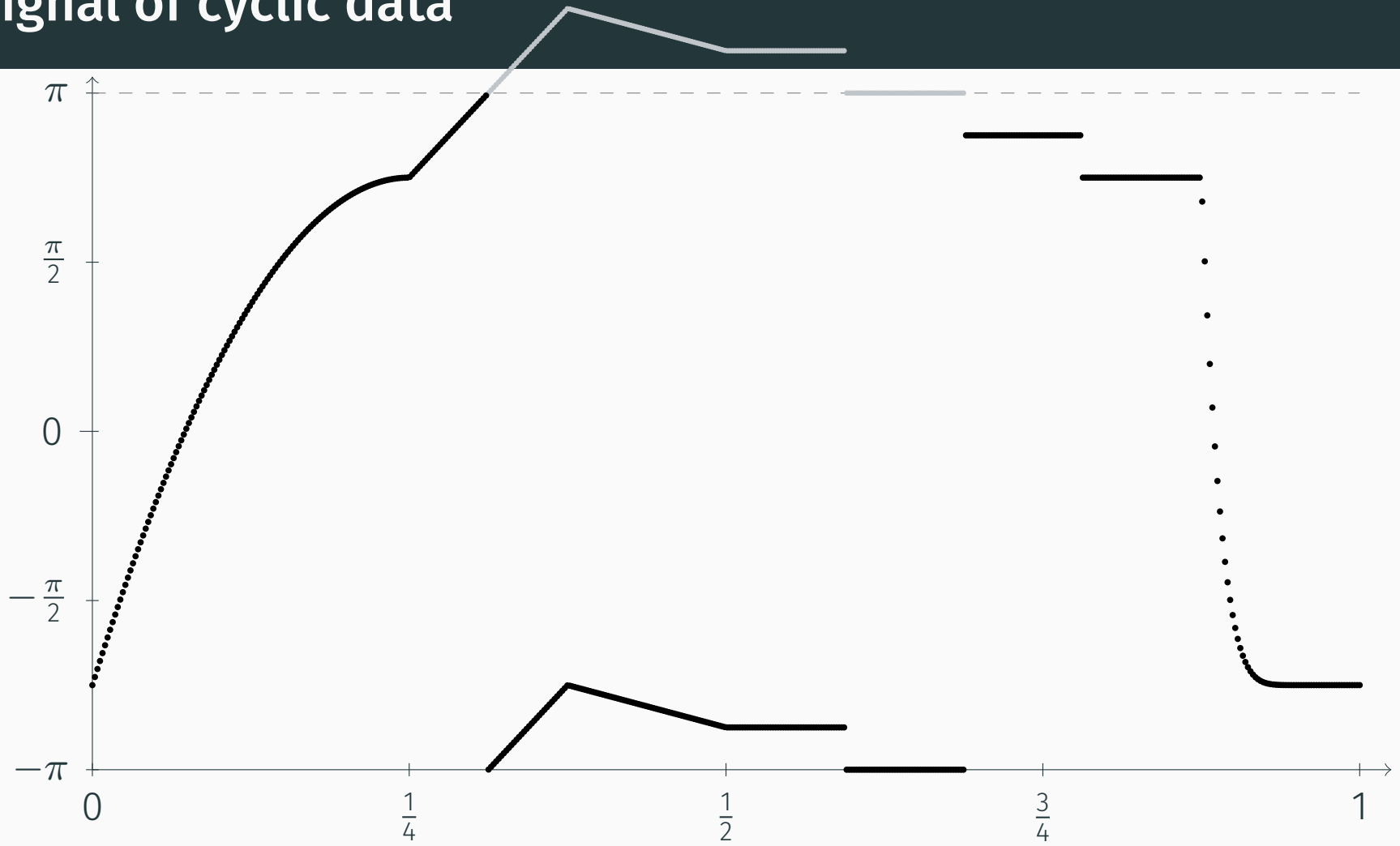

- function $f\colon [0,1] \to \mathbb{S}^1$ sampled to obtain data $f_0 = (f_{0,i})_{i=1}^{500}$
- f could be a wrapped version of the gray plot, hence
- jumps $> \pi$ at $\frac{5}{16}$ and $\frac{11}{16}$ are due to the representation system

A signal of cyclic data

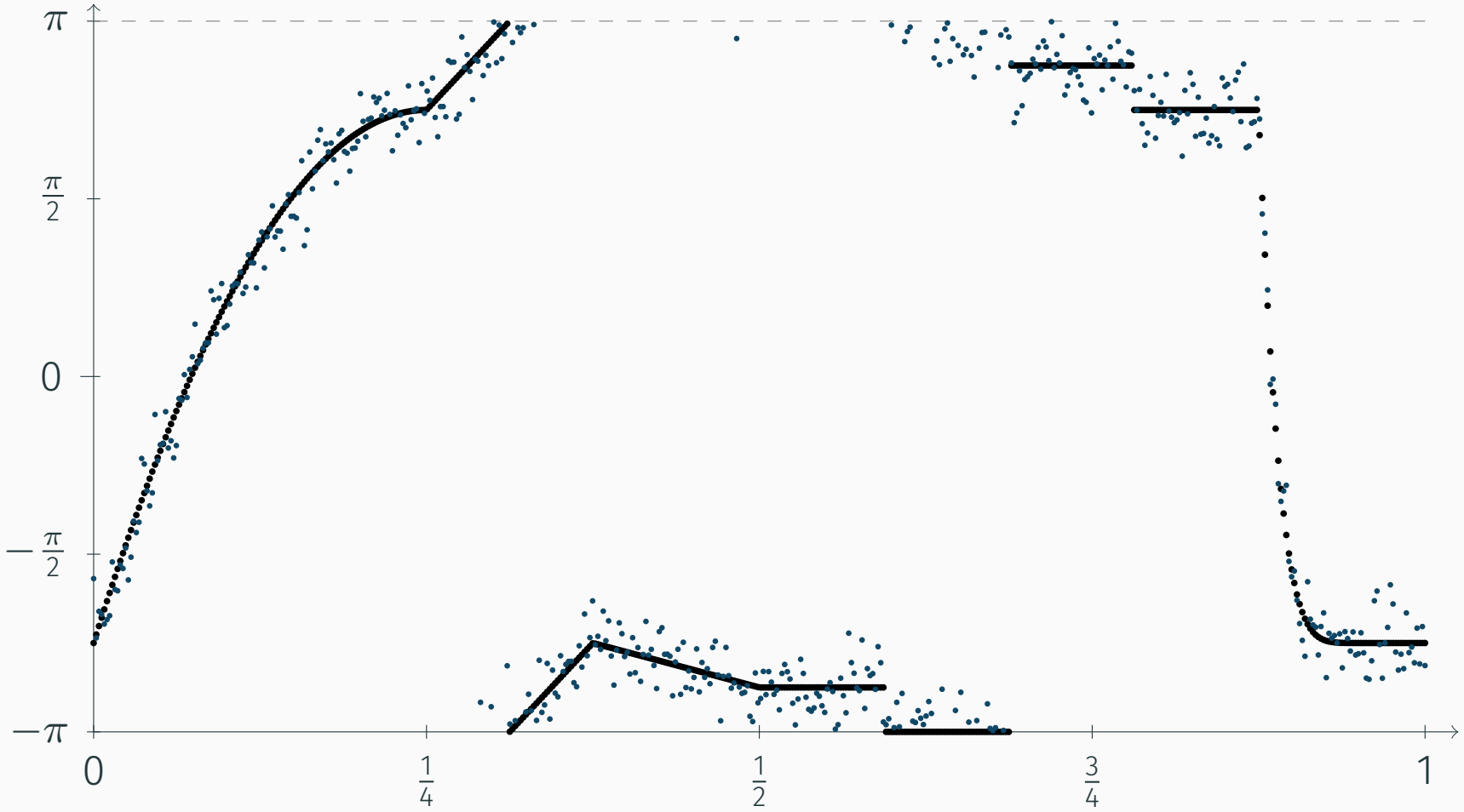

- function $f\colon [0,1] \to \mathbb{S}^1$ sampled to obtain data $f_{\mathrm{o}} = (f_{\mathrm{o},i})_{i=1}^{500}$
- adding wrapped Gaussian noise, $\sigma = 0.2$
- noisy data $f_{\mathrm{n}} = (f_{\mathrm{o}} + \eta)_{2\pi}$

A signal of cyclic data

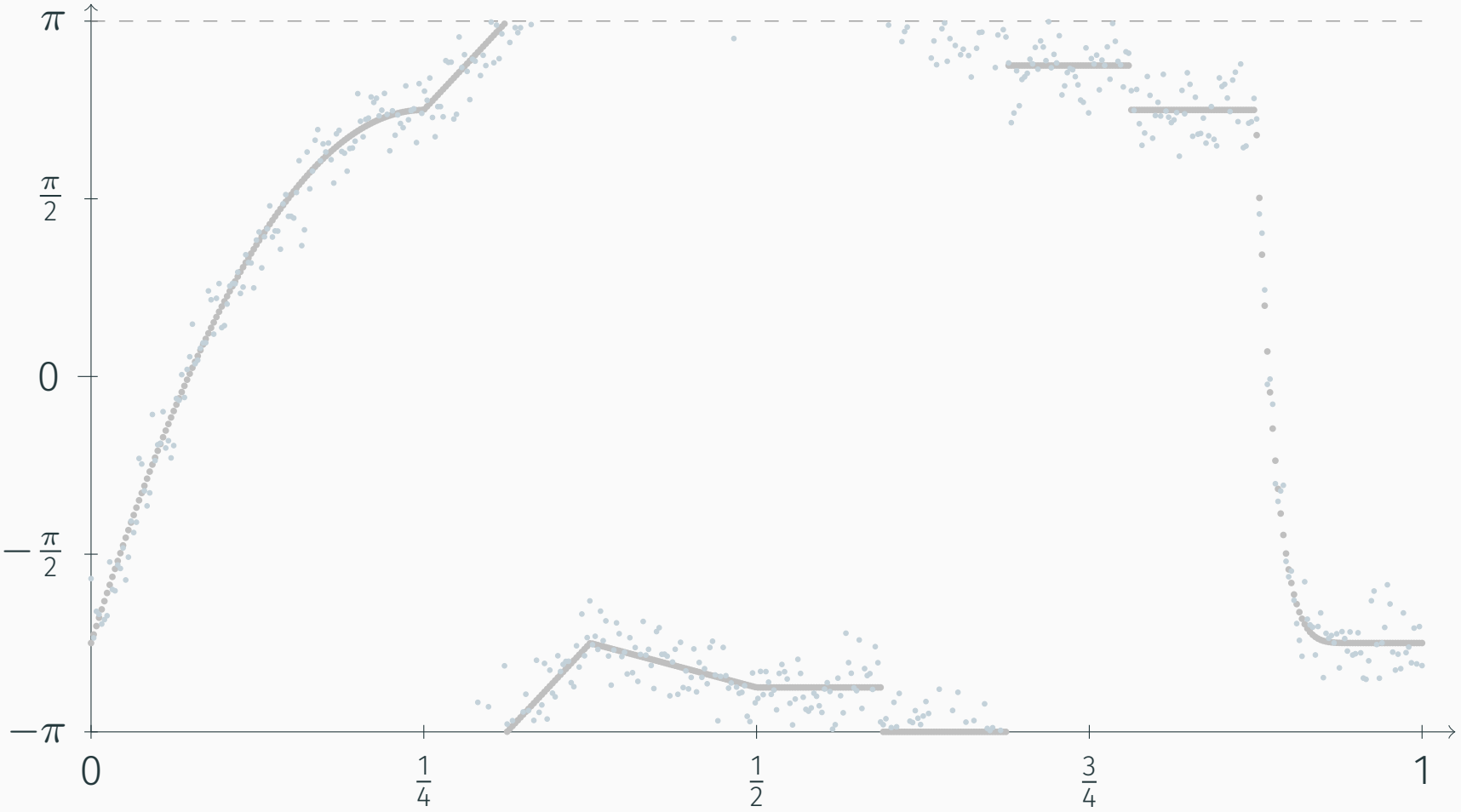

- comparison of f_o & f_n with

A signal of cyclic data

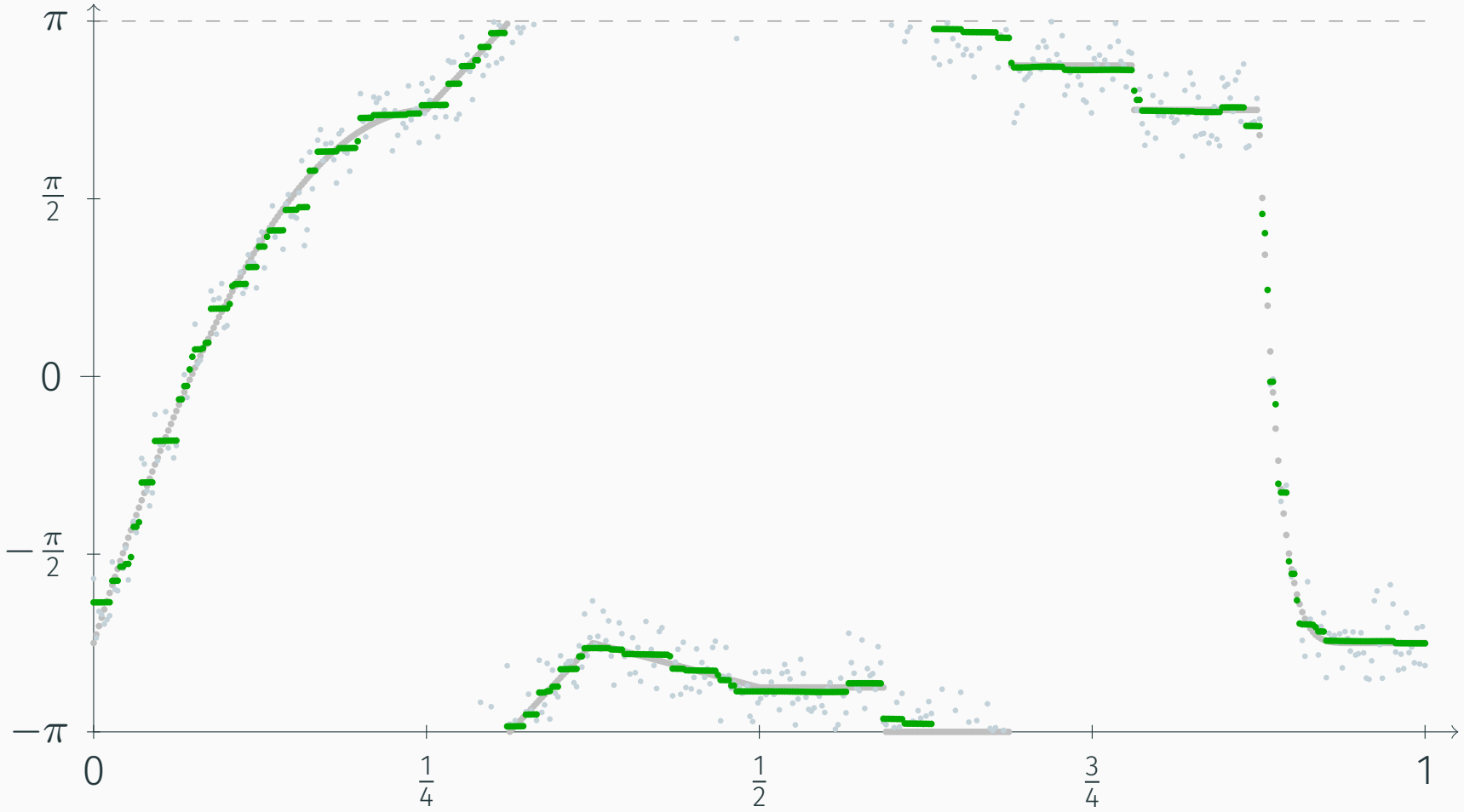

- comparison of f_0 & f_n with f_1
- denoising TV_1 ($\alpha = \frac{3}{4}$, $\beta = 0$)
- but: stair casing

A signal of cyclic data

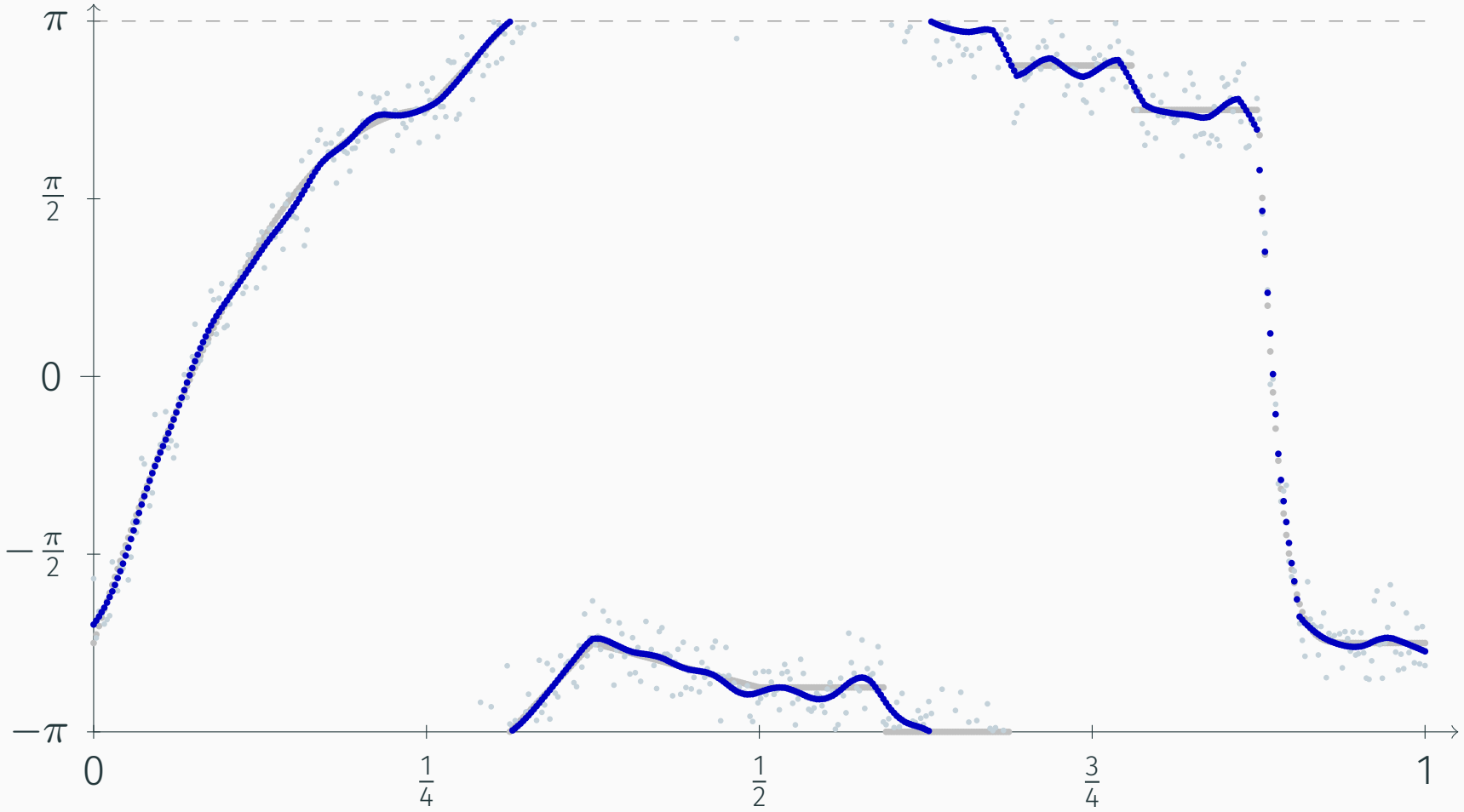

- comparison of f_0 & f_n with f_2
- denoising TV_2 ($\alpha = 0$, $\beta = \frac{3}{2}$)
- but: no plateaus

A signal of cyclic data

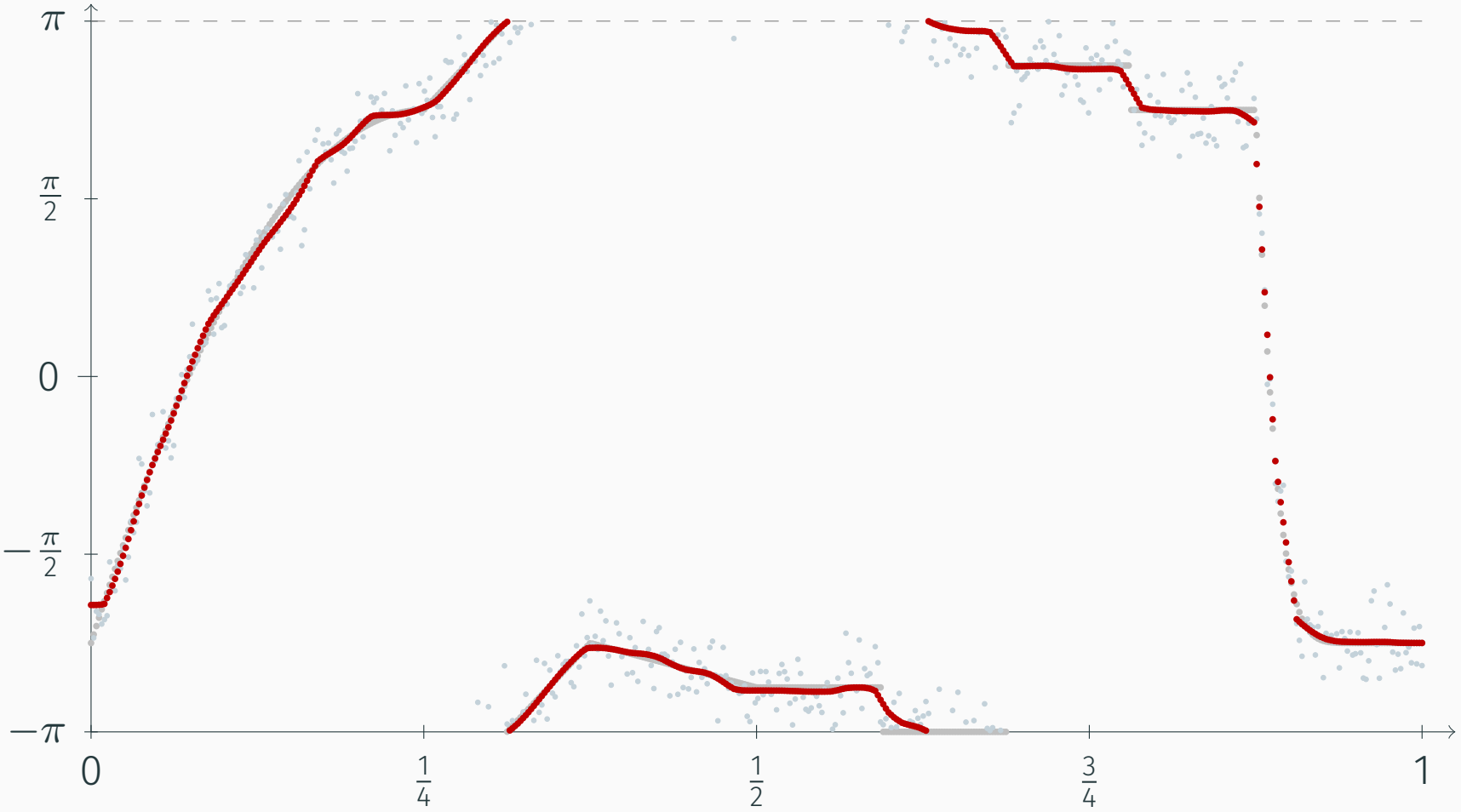

- comparison of f_0 & f_n with f_3
- denoising TV_1 & TV_2 ($\alpha = \frac{1}{2}$, $\beta = 1$)
- smallest mean squared error

Bernoulli's Lemniscate on the sphere $\mathbb{S}^2$

$$\gamma(t) := \frac{a\sqrt{2}}{\sin^2(t)+1}\big(\cos(t), \cos(t)\sin(t)\big)^{\mathrm{T}}, \quad t \in [0, 2\pi], a = \frac{\pi}{2\sqrt{2}}.$$

Generate a **sphere-valued signal** by putting it into the tangential plane of the north pole

$$\gamma_S(t) = \exp_p(\gamma(t)), p = (0, 0, 1)^{\mathrm{T}}$$

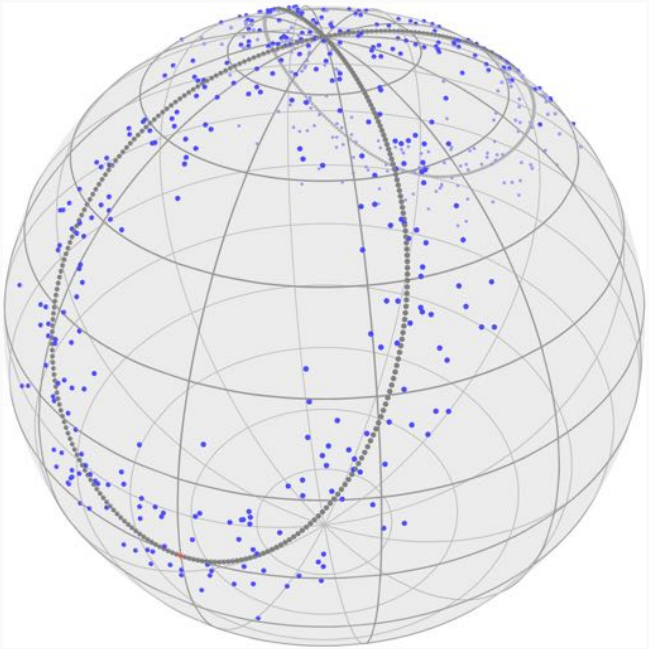

noisy lemniscate of Bernoulli on $\mathbb{S}^2$, Gaussian noise, $\sigma = \frac{\pi}{30}$, on $T_p\mathbb{S}^2$.

Bernoulli's Lemniscate on the sphere $\mathbb{S}^2$

$$\gamma(t) := \frac{a\sqrt{2}}{\sin^2(t)+1}\big(\cos(t), \cos(t)\sin(t)\big)^{\mathrm{T}}, \quad t \in [0, 2\pi], a = \frac{\pi}{2\sqrt{2}}.$$

Generate a **sphere-valued signal** by putting it into the tangential plane of the north pole

$$\gamma_S(t) = \exp_p(\gamma(t)), p = (0,0,1)^{\mathrm{T}}$$

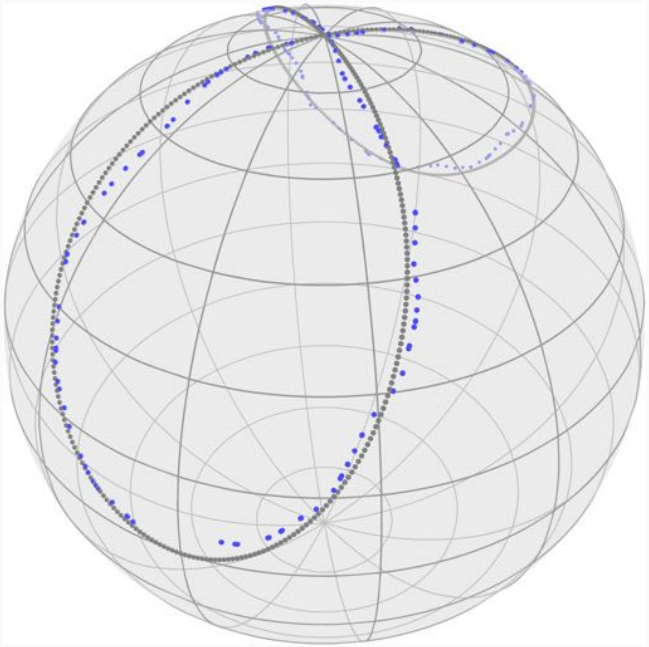

reconstruction with TV_1, $\alpha = 0.21$, $\mathrm{MAE} = 4.08 \times 10^{-2}$.

Bernoulli's Lemniscate on the sphere $\mathbb{S}^2$

$$\gamma(t) := \frac{a\sqrt{2}}{\sin^2(t)+1}\big(\cos(t), \cos(t)\sin(t)\big)^{\mathrm{T}}, \quad t \in [0, 2\pi], a = \frac{\pi}{2\sqrt{2}}.$$

Generate a **sphere-valued signal** by putting it into the tangential plane of the north pole

$$\gamma_S(t) = \exp_p(\gamma(t)), p = (0,0,1)^{\mathrm{T}}$$

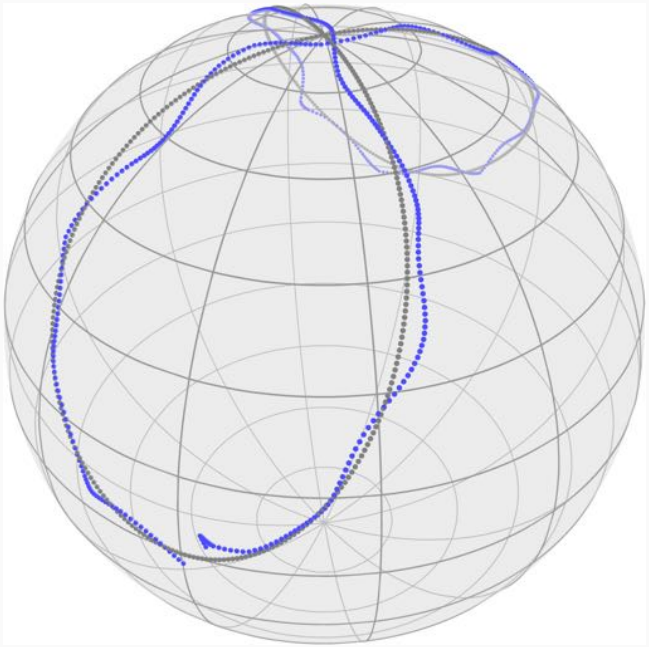

reconstruction with TV_2, $\alpha = 0$, $\beta = 10$, MAE $= 3.66 \times 10^{-2}$.

Bernoulli's Lemniscate on the sphere $\mathbb{S}^2$

$$\gamma(t) := \frac{a\sqrt{2}}{\sin^2(t)+1}\big(\cos(t), \cos(t)\sin(t)\big)^{\mathrm{T}}, \quad t \in [0, 2\pi], a = \frac{\pi}{2\sqrt{2}}.$$

Generate a **sphere-valued signal** by putting it into the tangential plane of the north pole

$$\gamma_S(t) = \exp_p(\gamma(t)), p = (0, 0, 1)^{\mathrm{T}}$$

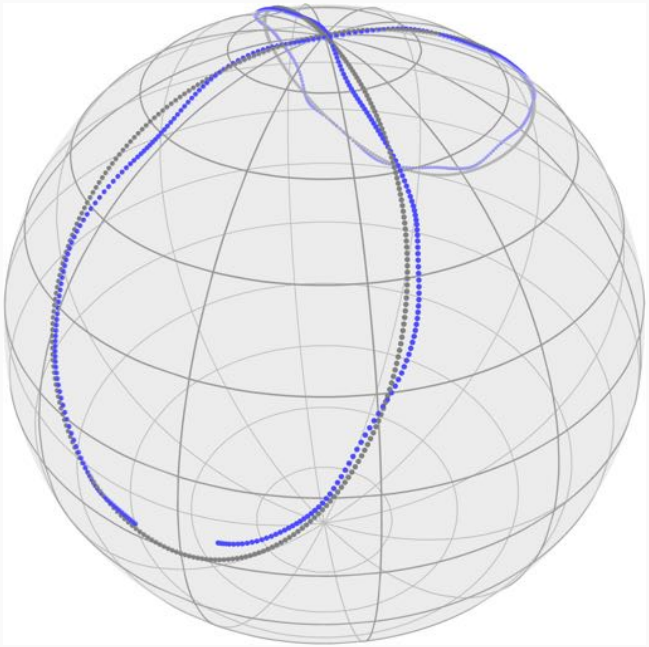

reconstruction with TV_1 & TV_2, $\alpha = 0.16$, $\beta = 12.4$, MAE $= 3.27 \times 10^{-2}$.

Inpainting of $\mathcal{P}(3)$-valued images

Draw symmetric positive definite 3×3 matrices as ellipsoids

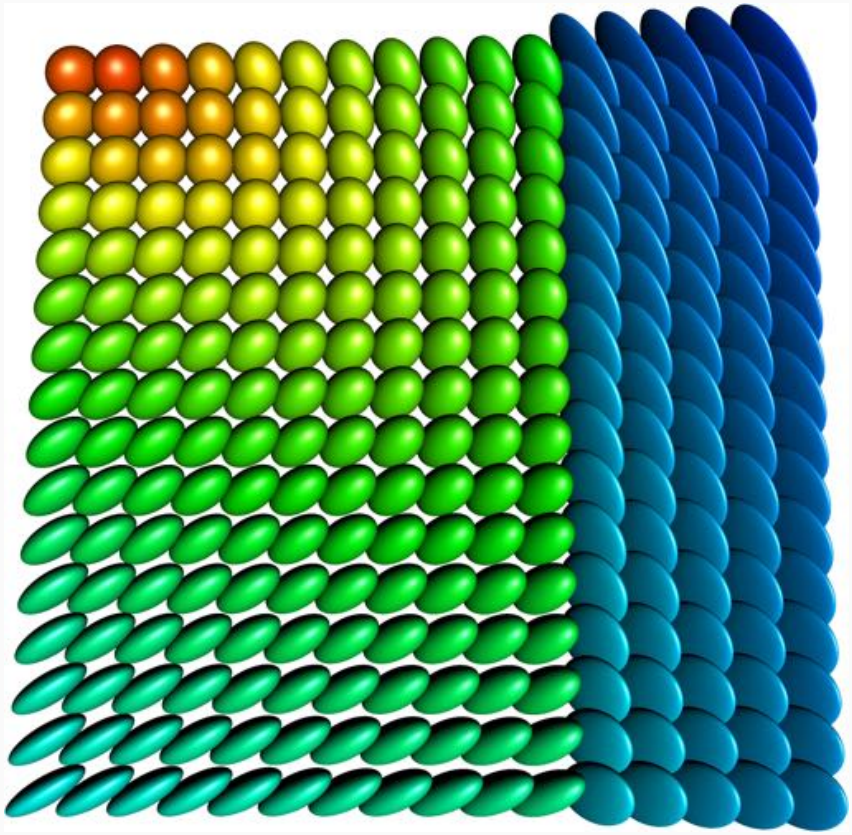

original data

Inpainting of $\mathcal{P}(3)$-valued images

Draw symmetric positive definite 3×3 matrices as ellipsoids

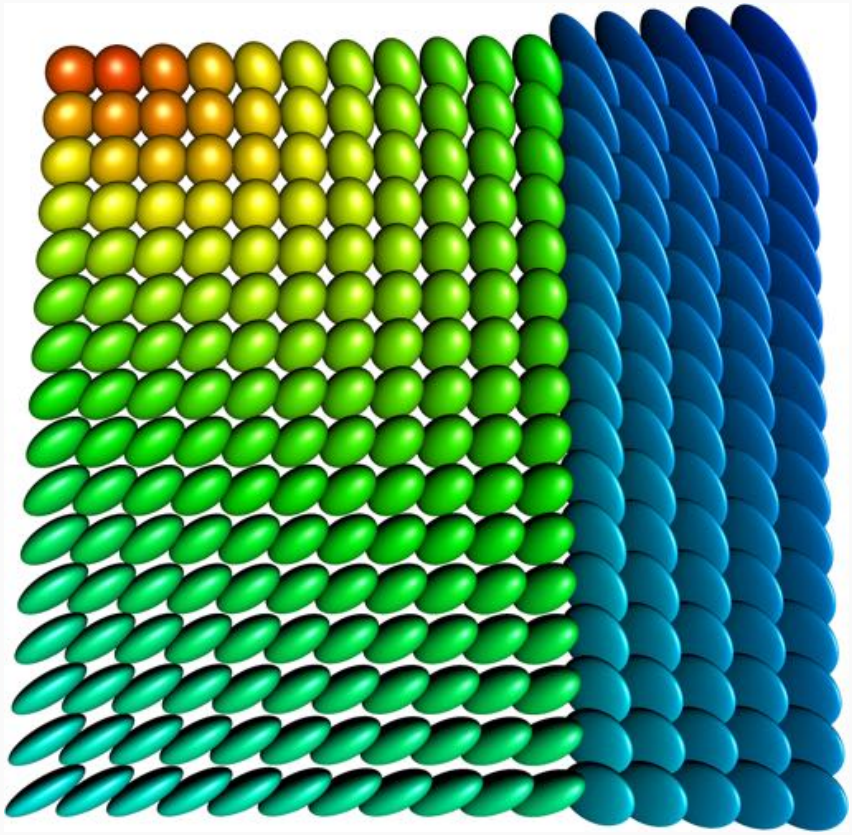

original data

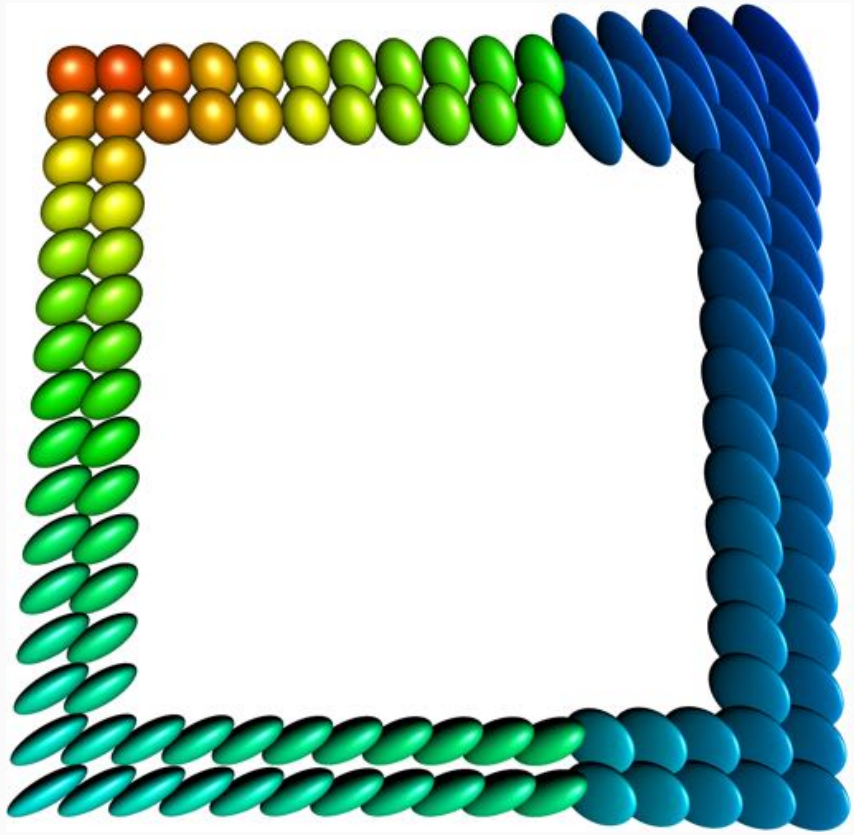

lost (a lot of) data

Inpainting of $\mathcal{P}(3)$-valued images

Draw symmetric positive definite 3×3 matrices as ellipsoids

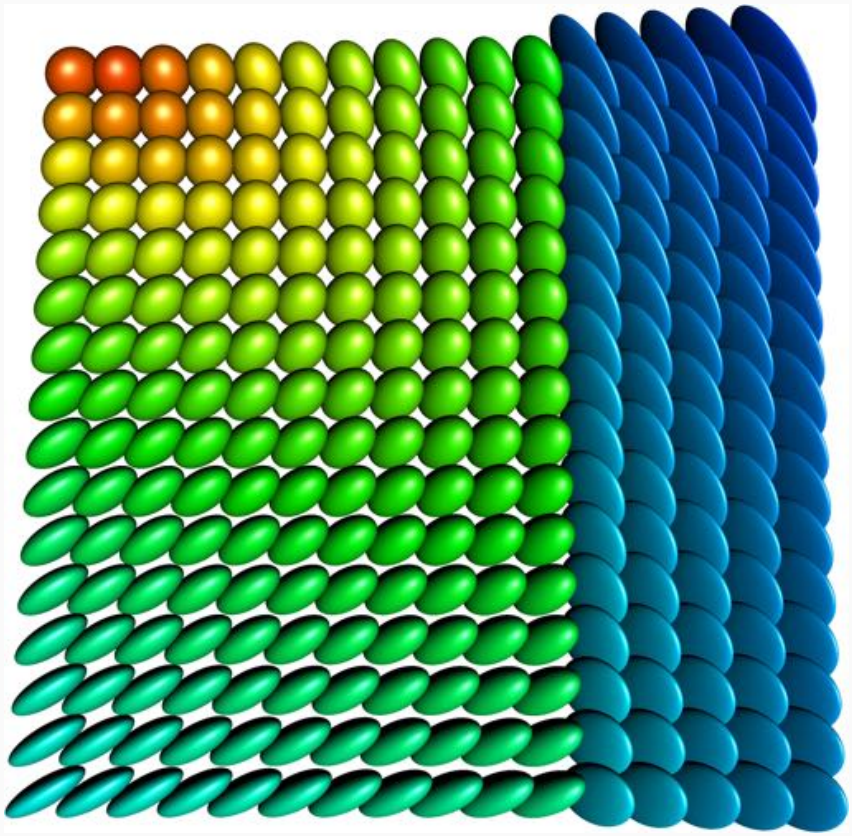

original data

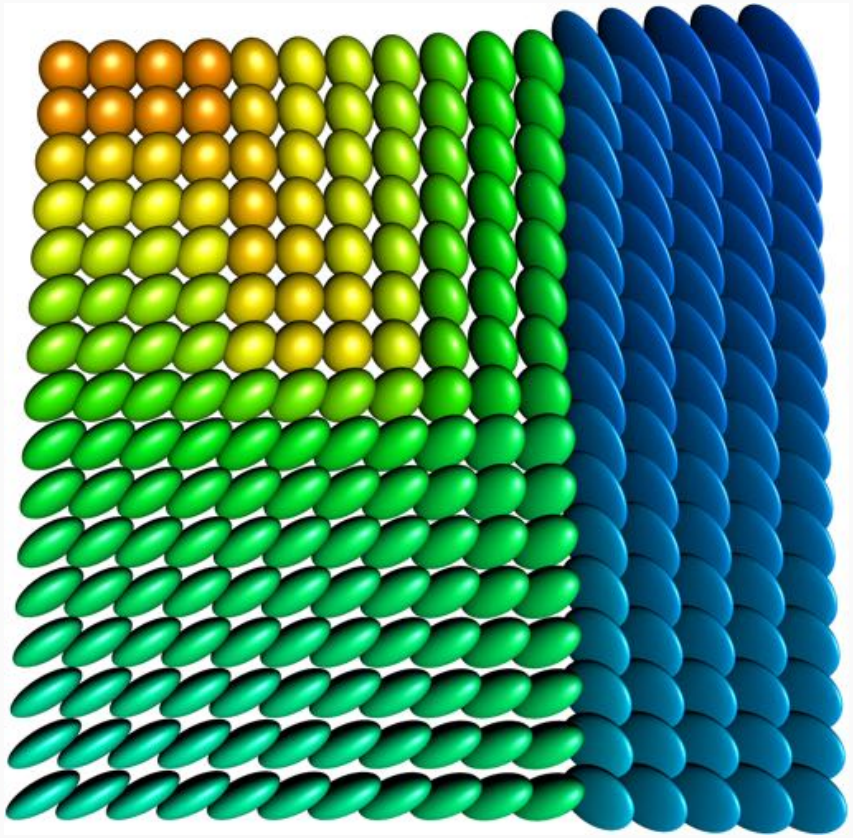

inpainted with $\alpha = \beta = 0.05$,
MAE $= 0.0929$

Inpainting of $\mathcal{P}(3)$-valued images

Draw symmetric positive definite 3×3 matrices as ellipsoids

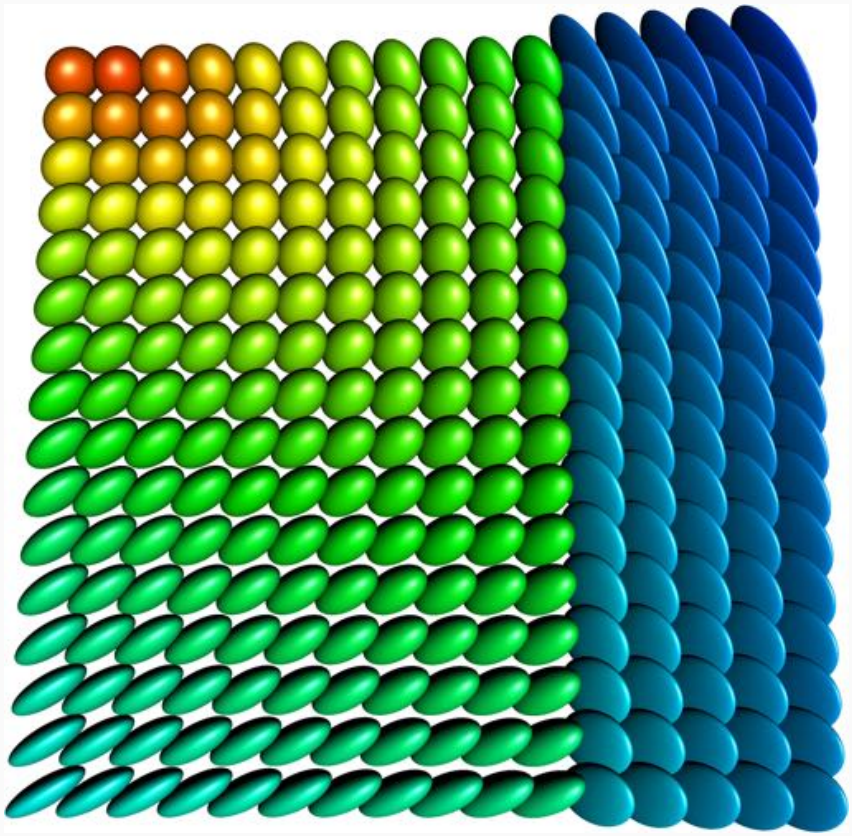

original data

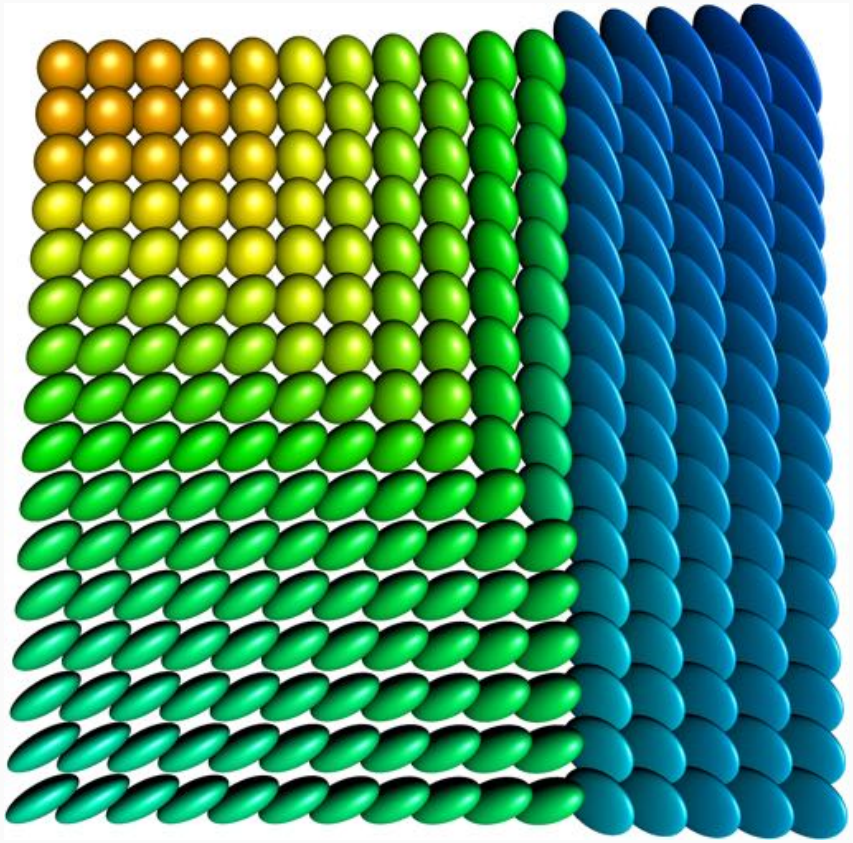

inpainted with $\alpha = 0.1$,
MAE $= 0.0712$

Properties and improvements

The cyclic proximal point algorithm is

- highly parallelizable
- very flexible
- known to converge (arbitrarily) slow

Improvements for first order TV

- parallel Douglas-Rachford algorithm: [RB, Persch, Steidl, 2016]
  only on Hadamard manifolds, faster convergence observed
- half-quadratic minimization: [RB, Chan, Hielscher, Persch, Steidl, 2016]
  relaxation and gradient descent or quasi-Newton.

Comparison of CPPA & PDRA

We compare number of iterations vs. value of the variational model function $\mathcal{E}(x^{(k)})$

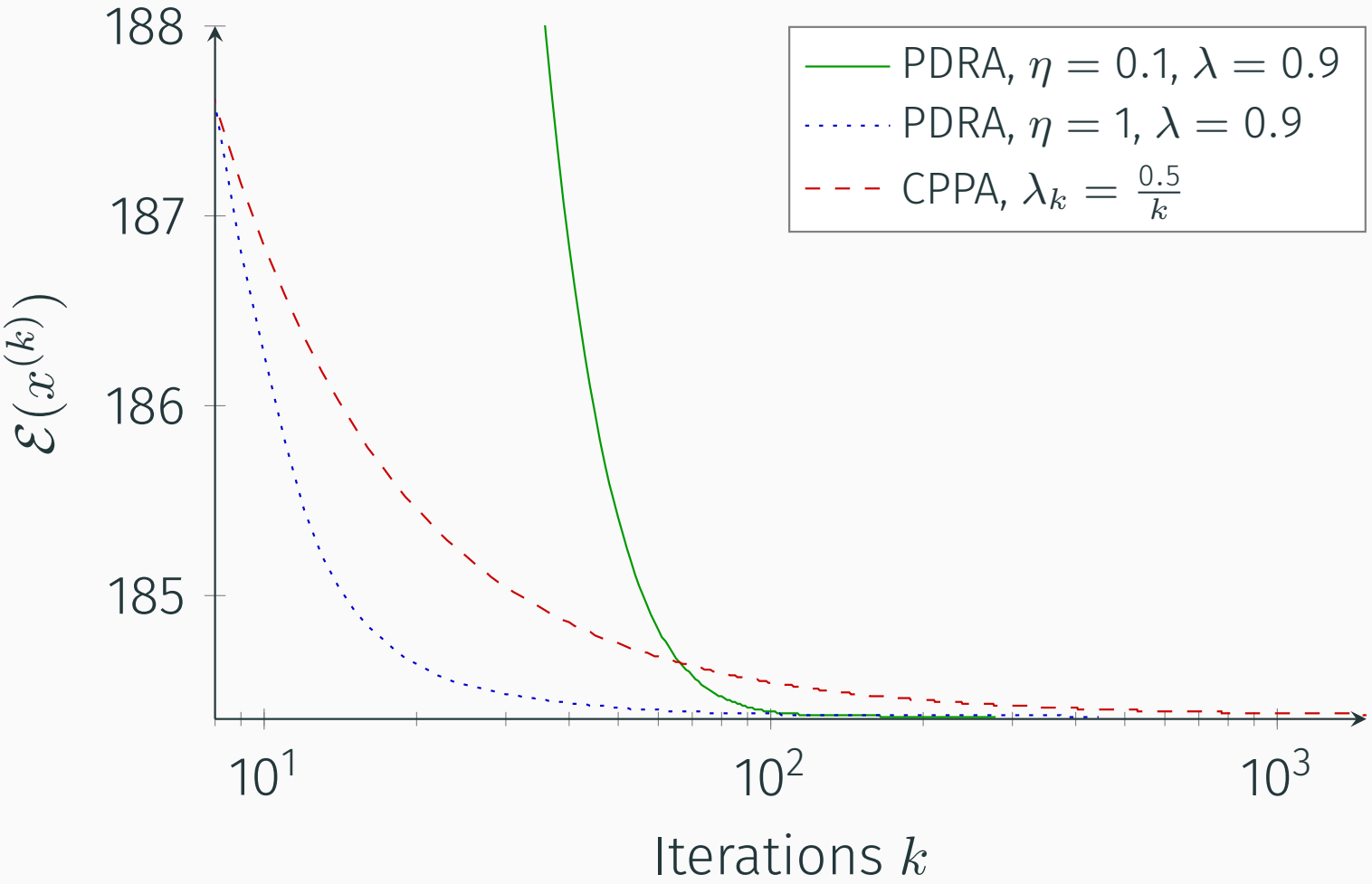

The graph p-Laplacian

Finite weighted graphs for image processing

A pixel might have a...

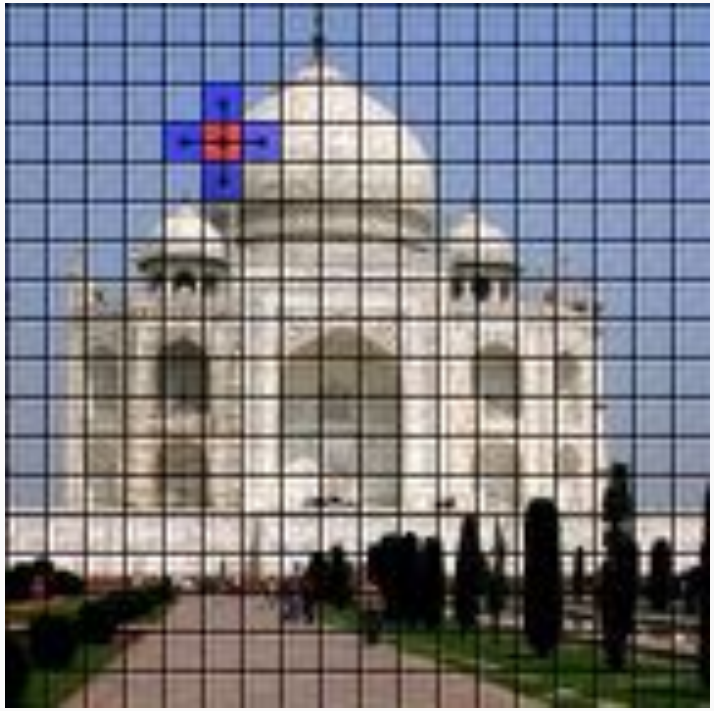

Local neighborhood

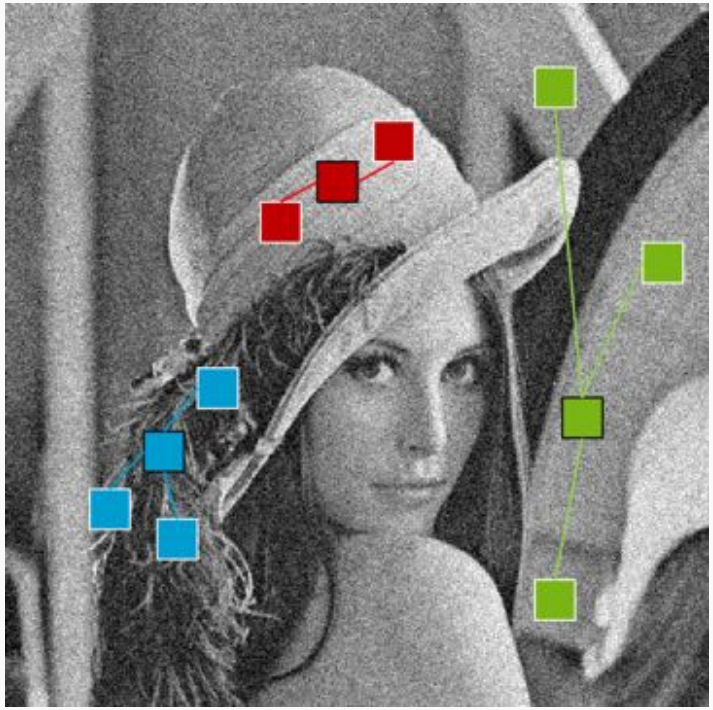

Nonlocal neighborhood

Finite weighted graphs for image processing

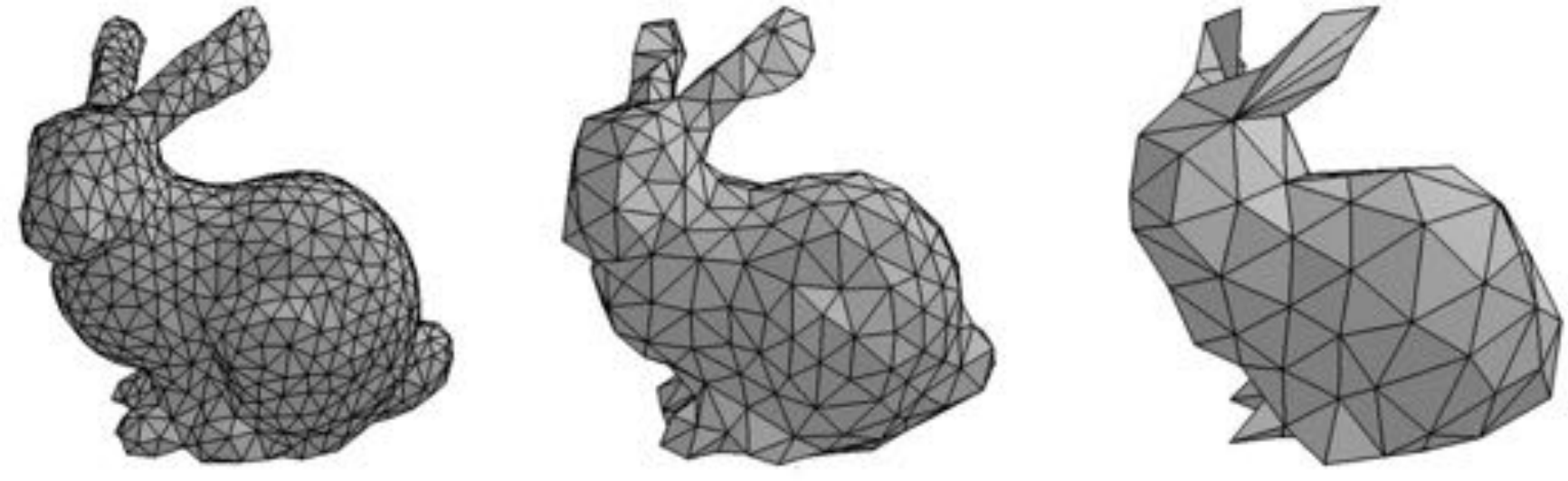

Polygon mesh approximation of a 3D surface. Image courtesy: Gabriel Peyré

"...Everything can be modeled as a graph"

The graph framework I

Let $G = (V, E, w)$ be a weighted (directed) graph, i.e.,

- V a finite set of nodes
- $E \subset V \times V$ a finite set of edges $(u, v) \in E$ short: $v \sim u$
- $w \colon V \times V \to \mathbb{R}^+$ a weight function with:
  $w(u, v) > 0 \Leftrightarrow (u, v) \in E$

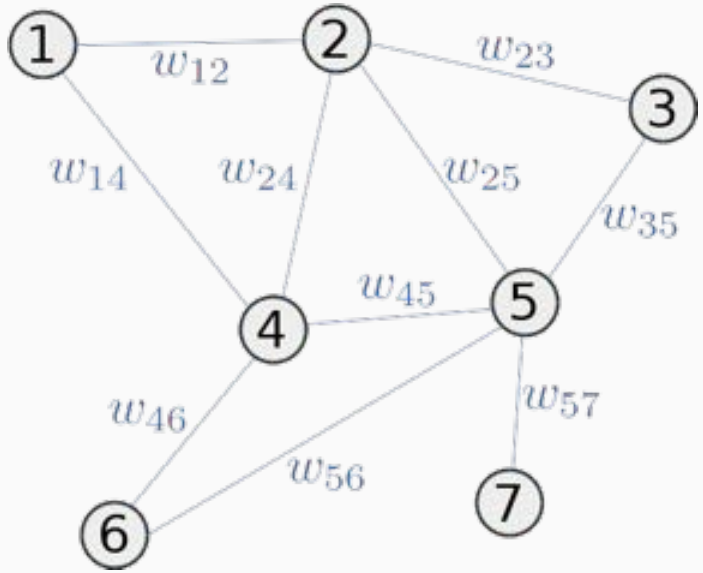

The graph framework II

Aim: Notion of a finite difference for data of **arbitrary topology**

[Almoataz, Lézoray, Bougleux, 2008]

$$\nabla f(u,v) = \sqrt{w(u,v)}\,\big(f(v) - f(u)\big)$$

Special case: Finite differences

Let $G = (V, E, w)$ be a directed 2-neighbour grid graph with the weight function w chosen as:

$$w(u,v) = \begin{cases} \frac{1}{h^2}\ , \text{ if } u \sim v \\ 0\ , \text{ else} \end{cases}$$

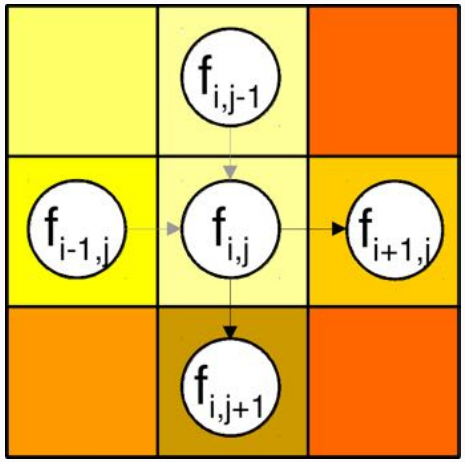

Translating higher order differential operators

Idea: Mimic important PDEs from image processing on finite weighted graphs, e.g., the p-Laplacian equation

[Elmoataz, Toutain, Tenbrinck, 2015]

Let $\Omega \subset \mathbb{R}^n$ an open, bounded set, let $1 \leq p < \infty$ and $f : \Omega \to \mathbb{R}^m$. We are interested in a solution of the **homogeneous p-Laplace equation**

$$\begin{aligned} \Delta_p f(x) &= -\operatorname{div}\left(\left\| \frac{\partial f}{\partial x_i} \right\|^{p-2} \frac{\partial f}{\partial x_i} \right)(x) \\ &= -\sum_{i=1}^{n} \left(\frac{\partial}{\partial x_i} \left\| \frac{\partial f}{\partial x_i} \right\|^{p-2} \frac{\partial f}{\partial x_i} \right)(x) = 0 \end{aligned}$$

Translating higher order differential operators

Idea: Mimic important PDEs from image processing on finite weighted graphs, e.g., the p-Laplacian equation

[Elmoataz, Toutain, Tenbrinck, 2015]

Let $G(V, E, w)$ a finite weighted graph, let $1 \leq p < \infty$ and $f : V \to \mathbb{R}^m$ a vertex function. We are interested in a solution of the following **finite difference equation**:

$$\begin{aligned}\Delta_{w,p} f(u) &= \frac{1}{2} \operatorname{div}\left(\|\nabla f\|^{p-2} \nabla f\right)(u) \\ &= -\sum_{v \sim u} (w(u,v))^{p/2} \|f(v) - f(u)\|^{p-2} (f(v) - f(u)) \;=\; 0\end{aligned}$$

Can we do the same for
manifold-valued vertex functions $f : V \to \mathcal{M}$?

The basic idea

Real-valued case	Manifold-valued case
$\mathcal{H}(V;\mathbb{R}^m) = \{f : V \to \mathbb{R}^m\}$	$\mathcal{H}(V;\mathcal{M}) \coloneqq \{f : V \to \mathcal{M}\}$
Space of edge functions	
$\mathcal{H}(E;\mathbb{R}^m) = \{H : E \to \mathbb{R}^m, H(u,v) \in \mathbb{R}^m, (u,v) \in E\}$	$\mathcal{H}(E;T_f\mathcal{M}) = \{H_f : E \to \mathrm{T}\mathcal{M}, H_f(u,v) \to \mathrm{T}_{f(u)}\mathcal{M}, (u,v) \in E\}$
Gradient	
$\nabla f(u,v) = \sqrt{w(u,v)}\big(f(v) - f(u)\big)$	$\nabla f(u,v) \coloneqq \sqrt{w(u,v)}\log_{f(u)} f(v) \in T_{f(u)}\mathcal{M}$
Local variation	
$\lVert\nabla f\rVert^p_{p,f(u)} = \sum_{v\sim u}\sqrt{w(u,v)}^p \lVert f(v) - f(u)\rVert^p$	$\lVert\nabla f\rVert^p_{p,f(u)} \coloneqq \sum_{v\sim u}\sqrt{w(u,v)}^p d_{\mathcal{M}}(f(u),f(v))^p$

(Local) divergence

What is $\langle \nabla f, H \rangle = \langle f, \nabla^\star H \rangle$, $\nabla^\star = -\operatorname{div}$, on a manifold?

(Local) divergence

Theorem [RB, Tenbrinck, 2017]

For $f \in \mathcal{H}(V;\mathcal{M})$, $H_f \in \mathcal{H}(E;\mathrm{T}_f\mathcal{M})$, we have

$$\langle \nabla f, H_f \rangle_{\mathcal{H}(E;\mathrm{T}_f\mathcal{M})} = \sum_{u\in V}\sum_{v\sim u} \langle \log_{f(u)} f(v), -\operatorname{div} H_f(u)\rangle_{f(u)},$$

where the **local divergence** is given by

$$\operatorname{div} H_f(u) := \frac{1}{2}\sum_{v\sim u} \sqrt{w(v,u)}\,\mathrm{PT}_{f(v)\to f(u)}\, H_f(v,u) - \sqrt{w(u,v)} H_f(u,v)$$

Remark

By antisymmetry $\nabla f(u,v) = -\mathrm{PT}_{f(v)\to f(u)}\,\nabla f(v,u) \in \mathrm{T}_{f(u)}\mathcal{M}$ we get

$$\operatorname{div}(\nabla f)(u) = -\sum_{v\sim u} w(u,v)\log_{f(u)} f(v)$$

The manifold-valued graph p-Laplacians

We define the **p-Graph-Laplacians**:

- **anisotropic** $\Delta_p^{\mathrm{a}}\colon \mathcal{H}(V;\mathcal{M}) \to \mathcal{H}(V;T\mathcal{M})$ by

$$\begin{aligned}\Delta_p^{\mathrm{a}} f(u) &:= \operatorname{div}\left(\|\nabla f\|_{f(\cdot)}^{p-2}\nabla f\right)(u)\\ &= -\sum_{v\sim u}\sqrt{w(u,v)}^{p} d_{\mathcal{M}}^{p-2}(f(u),f(v))\log_{f(u)} f(v)\end{aligned}$$

- **isotropic** $\Delta_p^{\mathrm{i}}\colon \mathcal{H}(V;\mathcal{M}) \to \mathcal{H}(V;T\mathcal{M})$ by

$$\begin{aligned}\Delta_p^{\mathrm{i}} f(u) &:= \operatorname{div}\left(\|\nabla f\|_{2,f(\cdot)}^{p-2}\nabla f\right)(u)\\ &= -\, b_{\mathrm{i}}(u)\sum_{v\sim u} w(u,v)\log_{f(u)} f(v)\ ,\end{aligned}$$

where

$$b_{\mathrm{i}}(u) := \|\nabla f\|_{2,f(u)}^{p-2} = \left(\sum_{v\sim u} w(u,v)\, d_{\mathcal{M}}^2(f(u),f(v))\right)^{\frac{p-2}{2}}.$$

Variational optimization problems

Goal: A Minimizer of a variational model $\mathcal{E}\colon \mathcal{H}(V;\mathcal{M}) \to \mathbb{R}$
the **anisotropic** energy functional

[Lellmann, Strekalovskiy, Kötters, Cremers, '13; Weinmann, Demaret, Storath, '14; RB, Persch, Steidl, '16]

$$\mathcal{E}_{\mathrm{a}}(f) := \frac{\lambda}{2} \sum_{u \in V} d^2_{\mathcal{M}}(f_0(u), f(u)) + \frac{1}{p} \sum_{(u,v)\in E} \|\nabla f(u,v)\|^p_{f(u)},$$

and the **isotropic** energy functional

[RB, Chan, Hielscher, Persch, Steidl, '16]

$$\mathcal{E}_{\mathrm{i}}(f) := \frac{\lambda}{2} \sum_{u \in V} d^2_{\mathcal{M}}(f_0(u), f(u)) + \frac{1}{p} \sum_{u \in V} \left(\sum_{v \sim u} \|\nabla f(u,v)\|^2_{f(u)} \right)^{p/2}.$$

Optimality conditions

For $e \in \{\mathrm{a}, \mathrm{i}\}$ and any $u \in V$ we have for a minimizer

$$0 \overset{!}{=} \Delta_p^e f(u) - \lambda \log_{f(u)} f_0(u) \in \mathrm{T}_{f(u)}\mathcal{M}.$$

Algorithm I. Forward difference or explicit scheme:

$$f_{n+1}(u) = \exp_{f_n(u)}\left(\Delta t \left(\Delta_p^{\mathrm{e}} f_n(u) - \lambda \log_{f_n(u)} f_0(u)\right)\right)$$

! to meet CFL conditions: small Δt necessary

Algorithm II. Jacobi iteration

$$f_{n+1}(u) = \exp_{f_n(u)}\left(\frac{\sum_{v\sim u} b(u,v)\log_{f_n(u)} f_n(v) + \lambda \log_{f_n(u)} f_0(u)}{\lambda + \sum_{v\sim u} b(u,v)}\right),$$

$$b(u,v) = \begin{cases} \sqrt{w(u,v)}^p d_{\mathcal{M}}^{p-2}(f(u), f(v)), & e = \mathrm{a}, \\ b_{\mathrm{i}}(u), & e = \mathrm{i}. \end{cases}$$

Evolution for the graph p-Laplacian

- $\mathcal{M} = \mathbb{S}^2$
- $V = \{1, \dots, 64\} \times \{1, \dots, 64\}$ pixel grid
- E is the 4-neighborhood, Neumann boundary

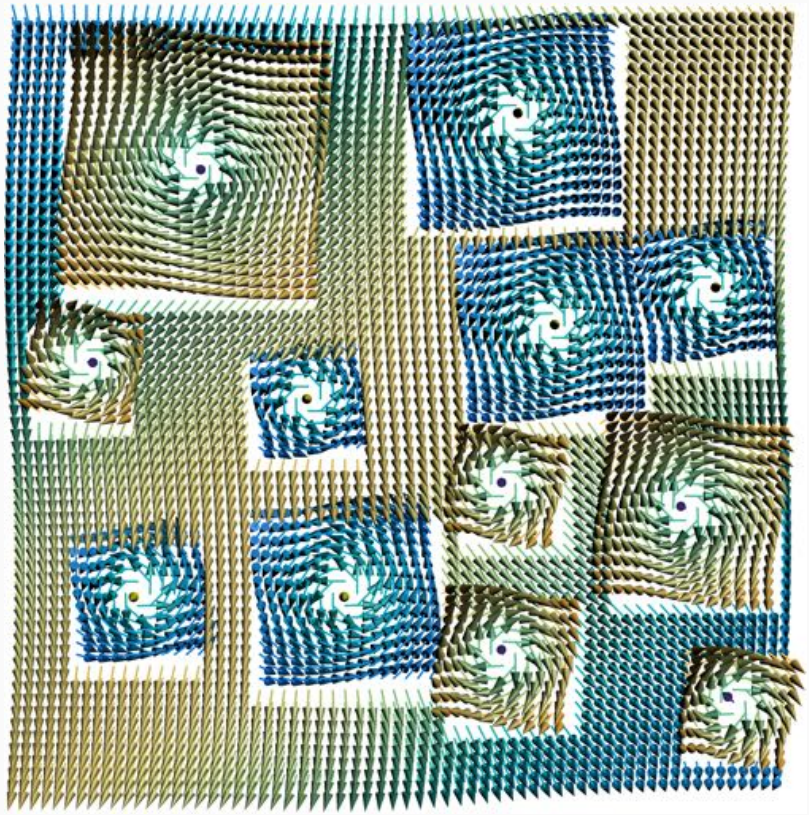

f_0

$\lambda = 0$ (no data term)

Evolution for the graph p-Laplacian

- $\mathcal{M} = \mathbb{S}^2$
- $V = \{1, \dots, 64\} \times \{1, \dots, 64\}$ pixel grid
- E is the 4-neighborhood, Neumann boundary

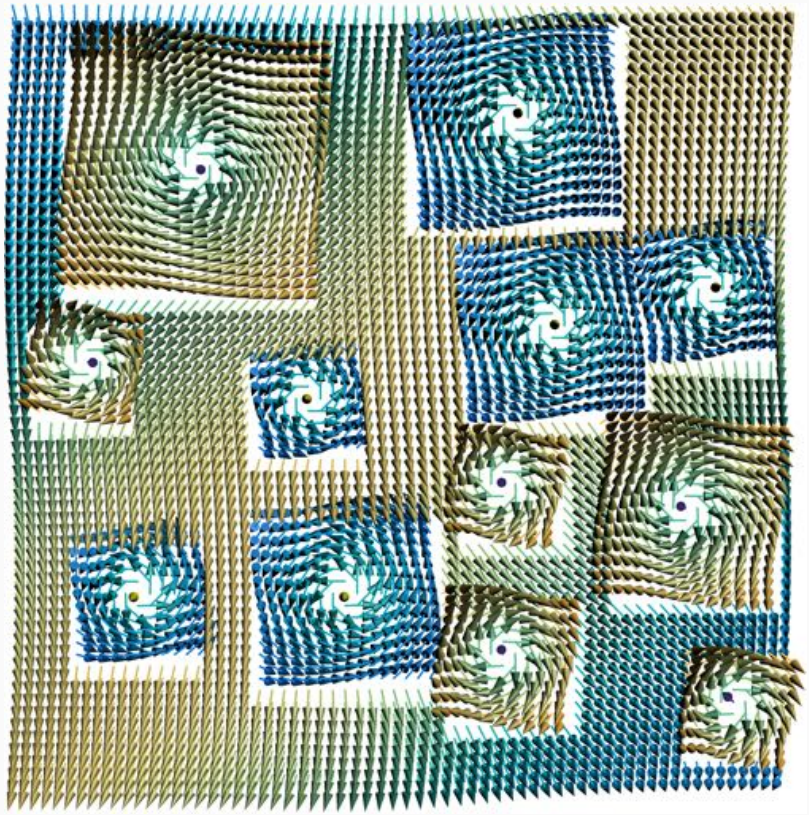

f_0

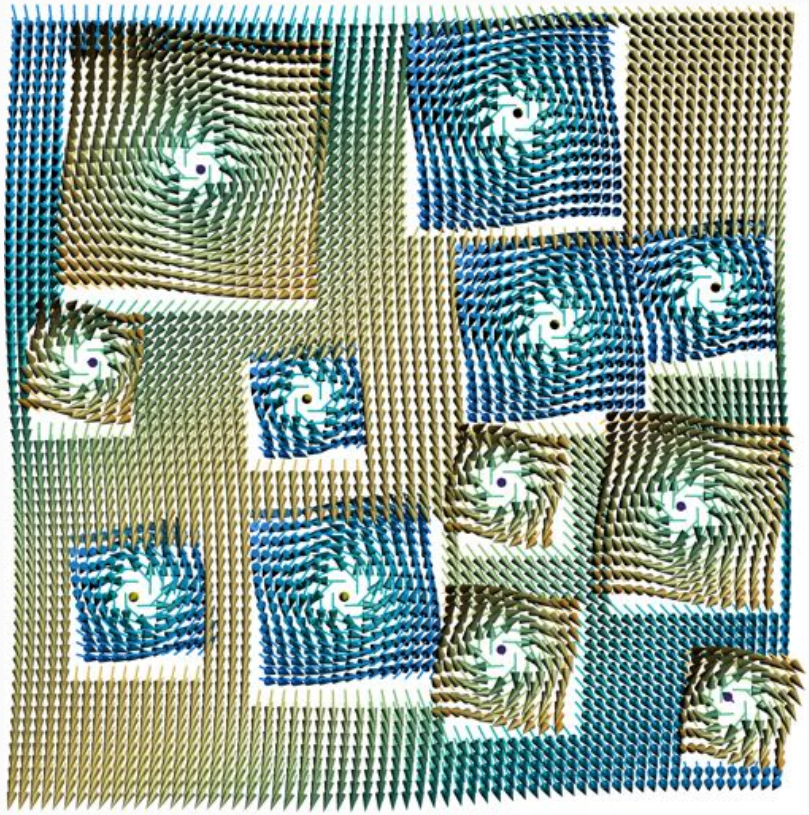

$\lambda = 0$, $p = 1$, anisotrop

Evolution for the graph p-Laplacian

- $\mathcal{M} = \mathbb{S}^2$
- $V = \{1, \dots, 64\} \times \{1, \dots, 64\}$ pixel grid
- E is the 4-neighborhood, Neumann boundary

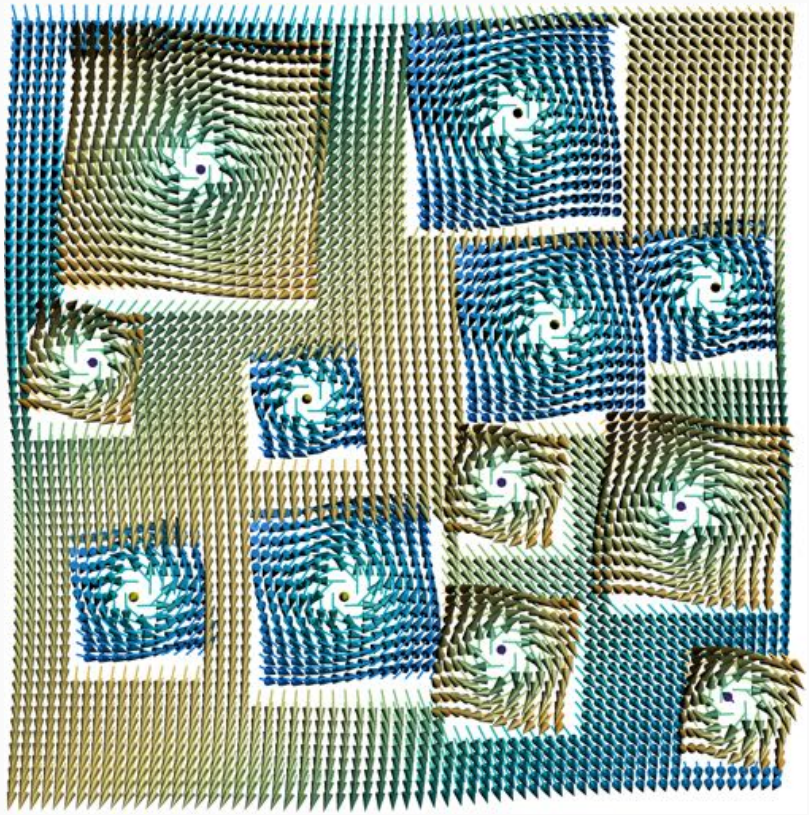

f_0

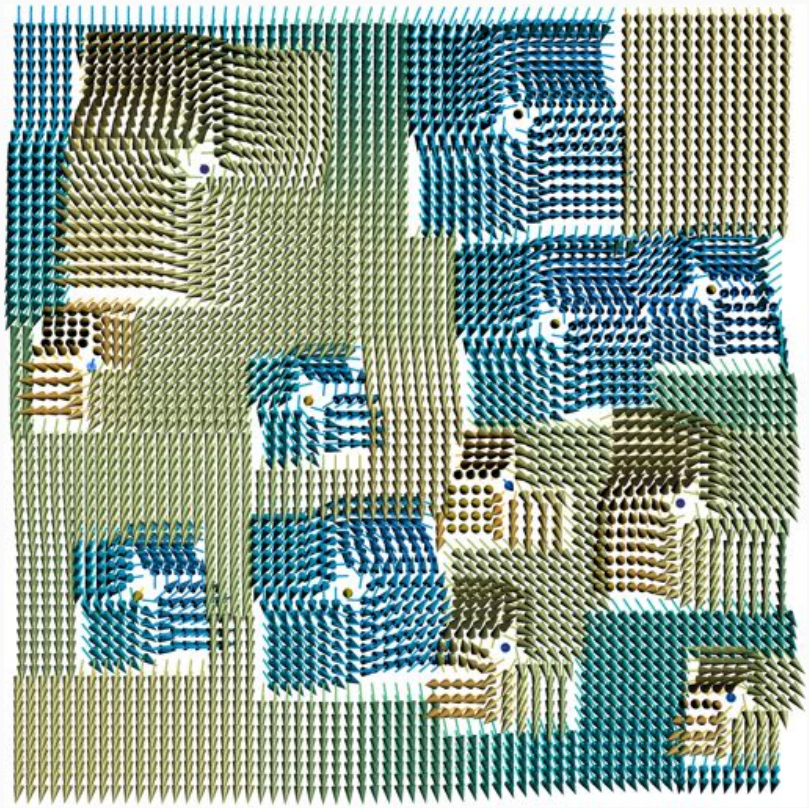

f_{1000}

$\lambda = 0$, $p = 1$, anisotrop

Evolution for the graph p-Laplacian

- $\mathcal{M} = \mathbb{S}^2$
- $V = \{1, \dots, 64\} \times \{1, \dots, 64\}$ pixel grid
- E is the 4-neighborhood, Neumann boundary

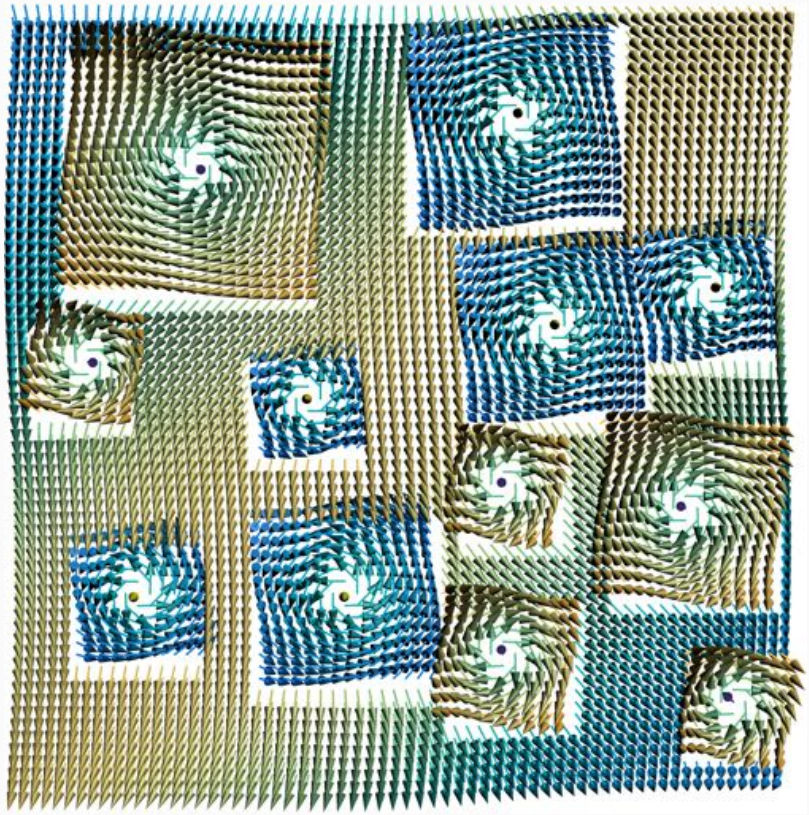

f_0

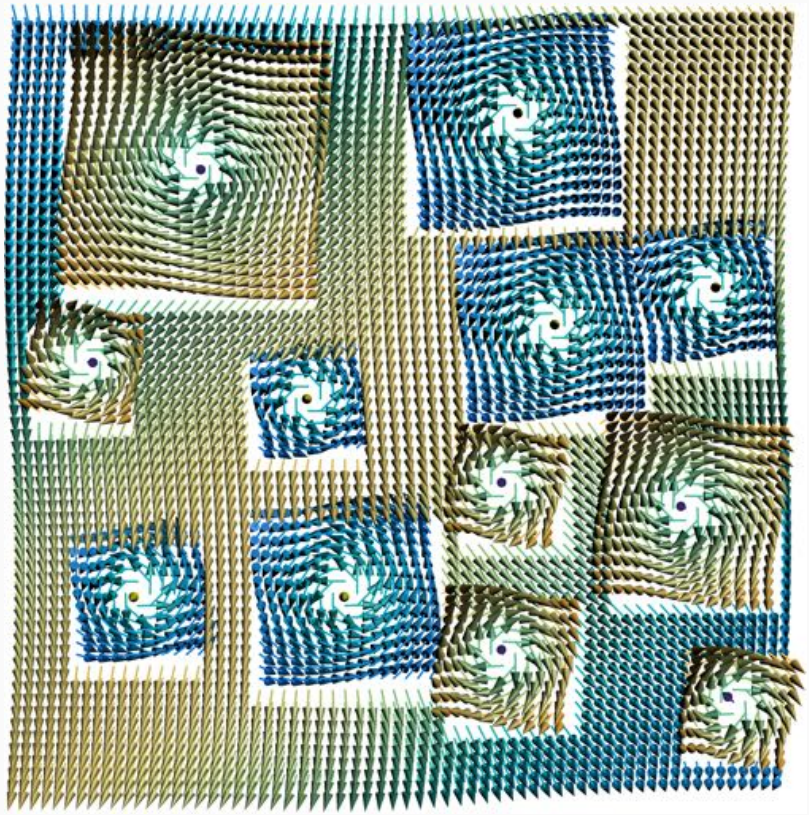

$\lambda = 0$, $p = 1$, isotrop

Evolution for the graph p-Laplacian

- $\mathcal{M} = \mathbb{S}^2$
- $V = \{1, \dots, 64\} \times \{1, \dots, 64\}$ pixel grid
- E is the 4-neighborhood, Neumann boundary

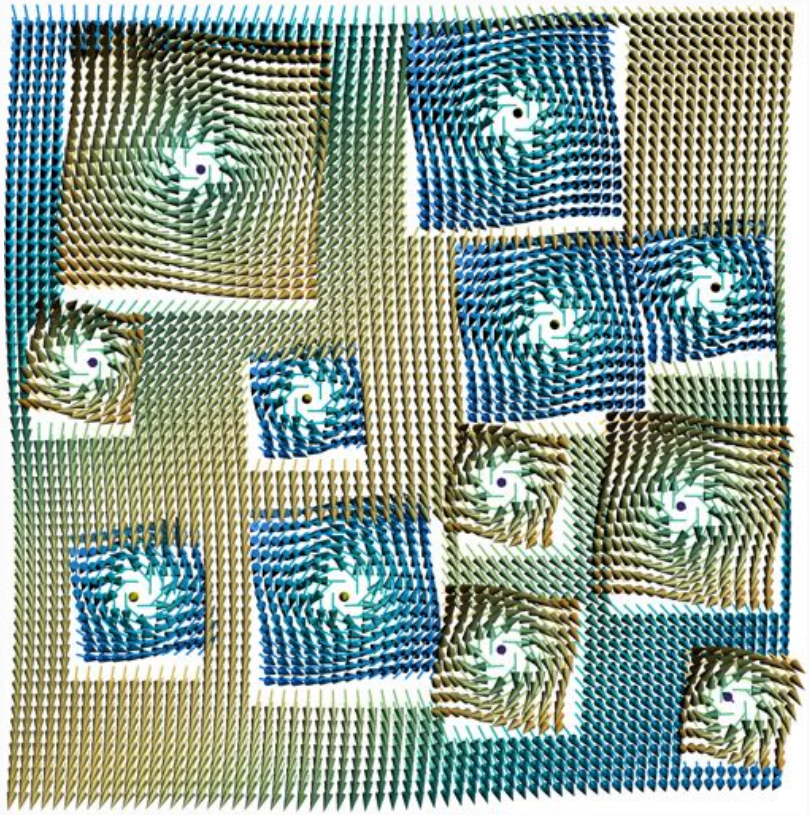

f_0

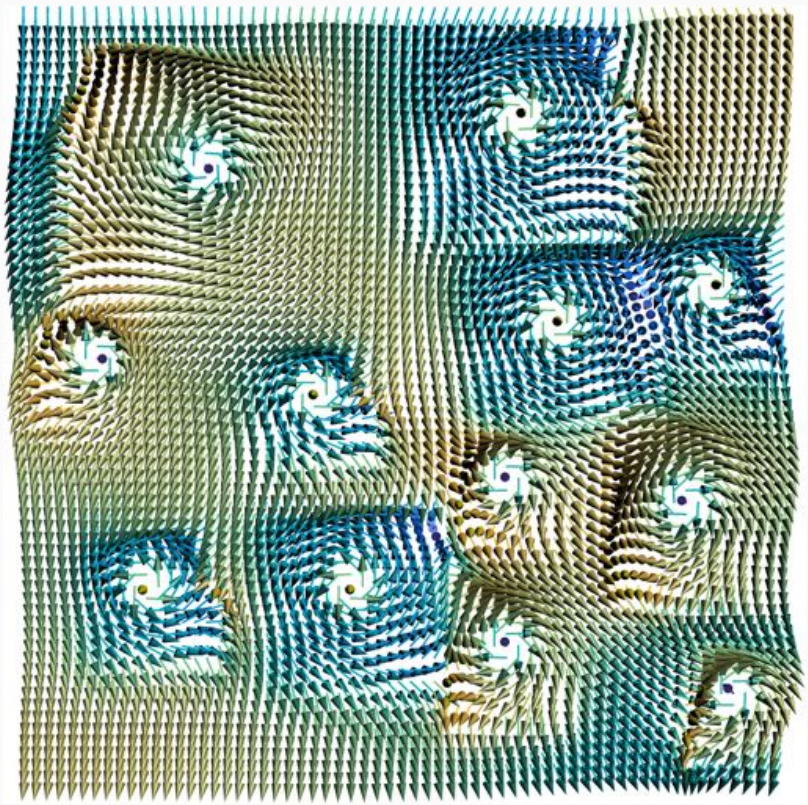

f_{1000}

$\lambda = 0$, $p = 1$, isotrop

Evolution for the graph p-Laplacian

- $\mathcal{M} = \mathbb{S}^2$
- $V = \{1, \dots, 64\} \times \{1, \dots, 64\}$ pixel grid
- E is the 4-neighborhood, Neumann boundary

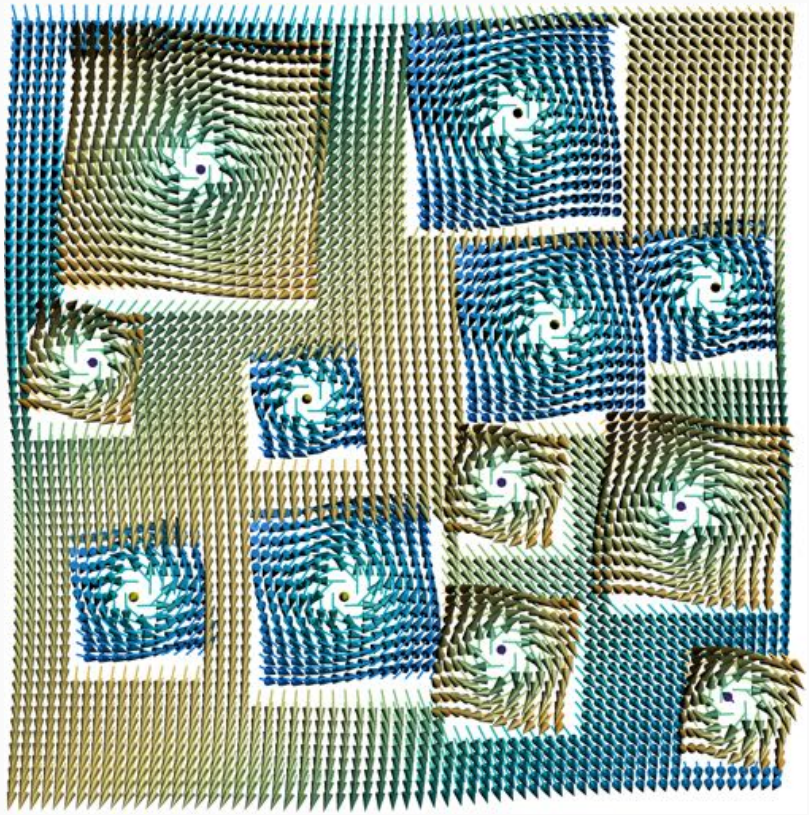

f_0

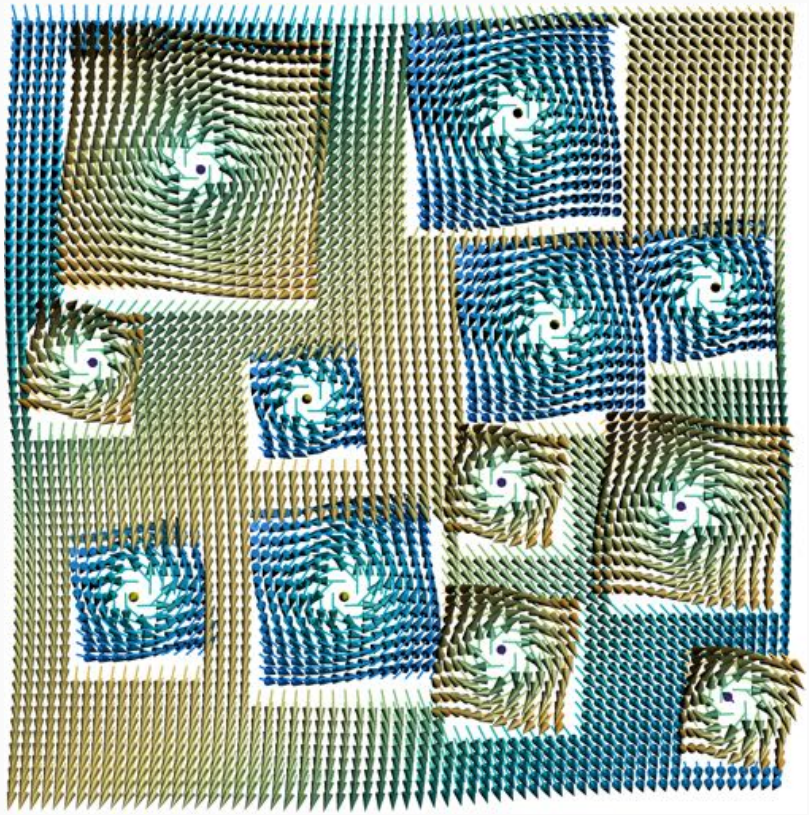

$\lambda = 0$, $p = 2$, (an)isotrop

Evolution for the graph p-Laplacian

- $\mathcal{M} = \mathbb{S}^2$
- $V = \{1, \dots, 64\} \times \{1, \dots, 64\}$ pixel grid
- E is the 4-neighborhood, Neumann boundary

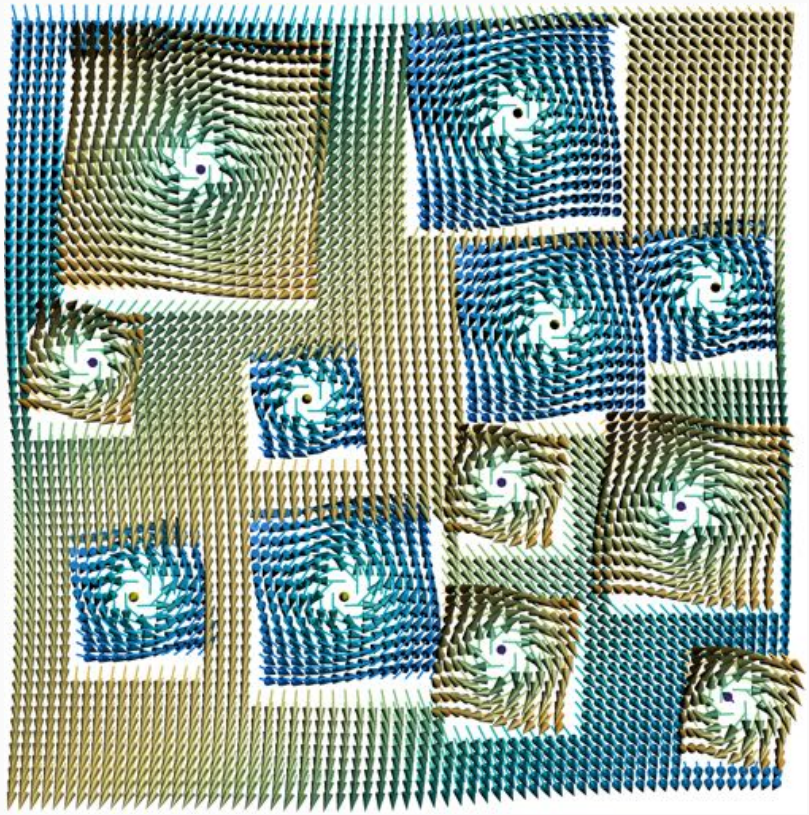

f_0

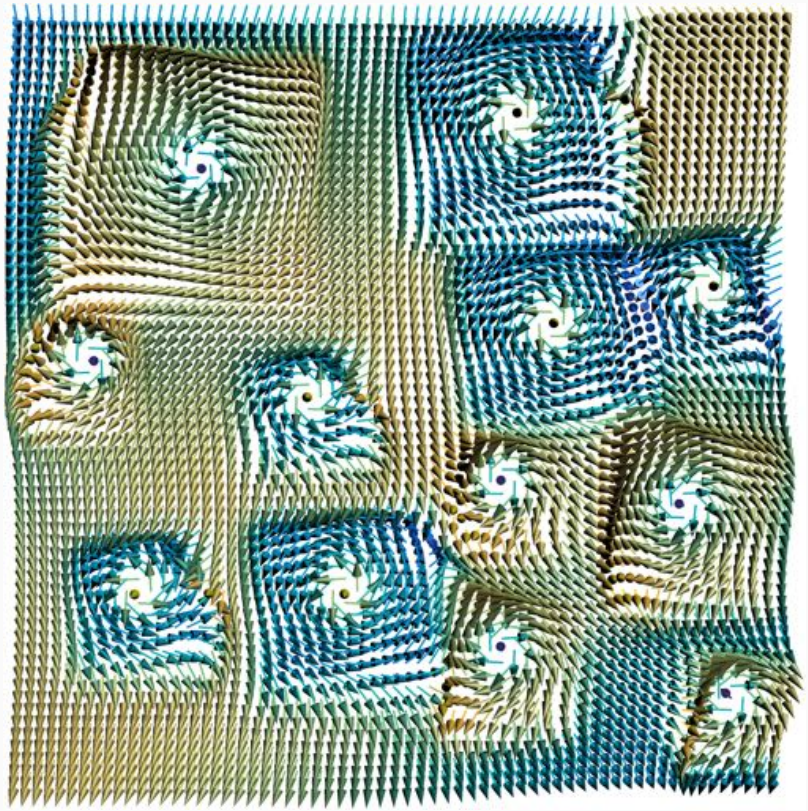

f_{1000}

$\lambda = 0$, $p = 2$, (an)isotrop

Evolution for the graph p-Laplacian

- $\mathcal{M} = \mathbb{S}^2$
- $V = \{1, \dots, 64\} \times \{1, \dots, 64\}$ pixel grid
- E is the 4-neighborhood, Neumann boundary

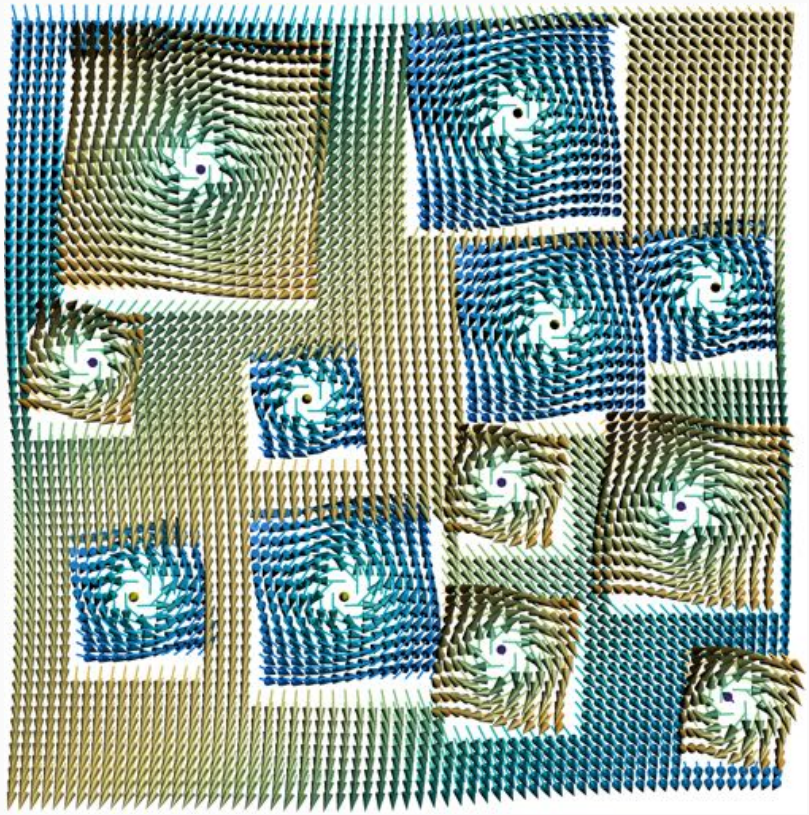

f_0

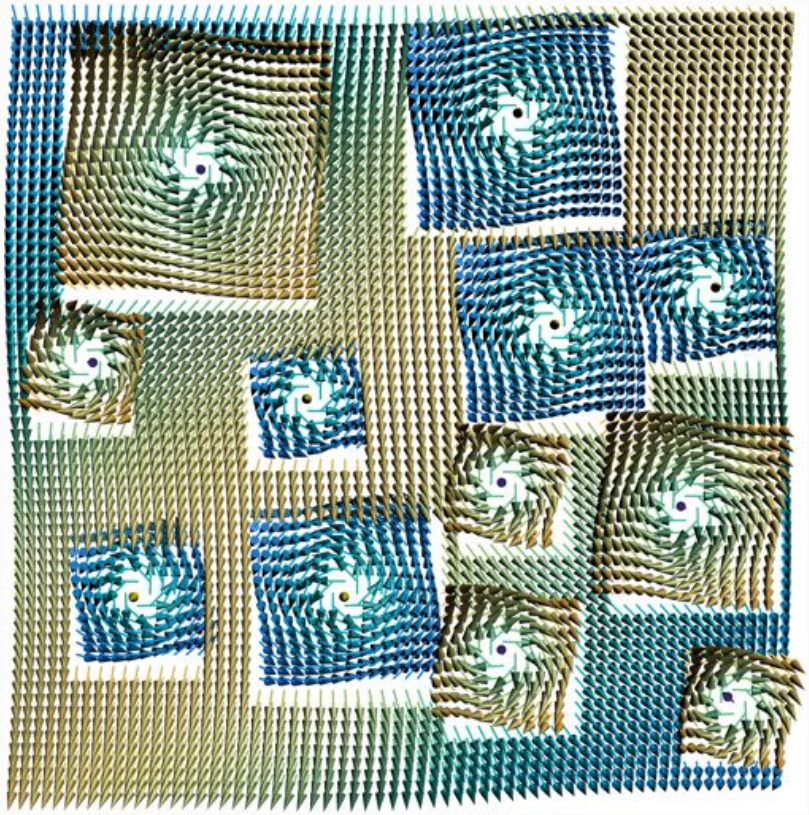

$\lambda = 1, p = 1$, anisotrop

Local image denoising

Light Detection and Ranging data (LiDaR), 40×40 pixel

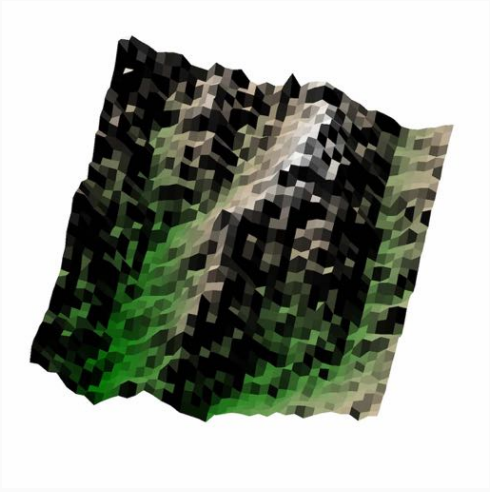

original data

[Geesch et al., 2009] via MFOPT
lellmann.net/software/mfopt

Local image denoising

Light Detection and Ranging data (LiDaR), 40×40 pixel

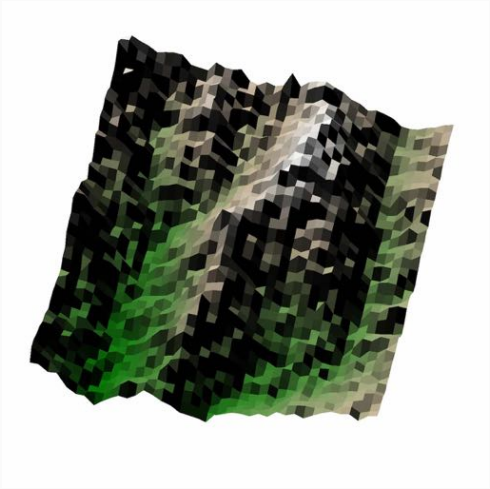

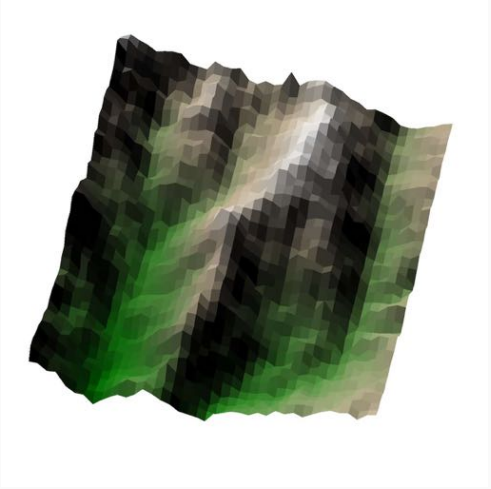

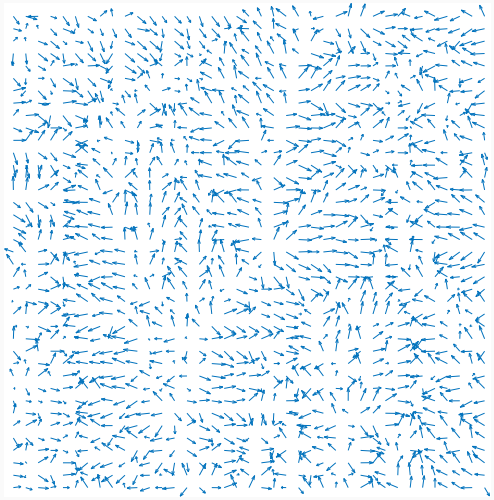

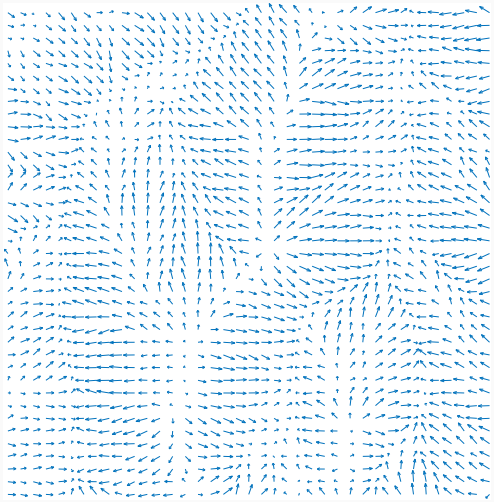

original data

[Geesch et al., 2009] via MFOPT
lellmann.net/software/mfopt

$p = 2$, $\lambda = 0.5$,
(an)isotrop.

Local image denoising

Light Detection and Ranging data (LiDaR), 40×40 pixel

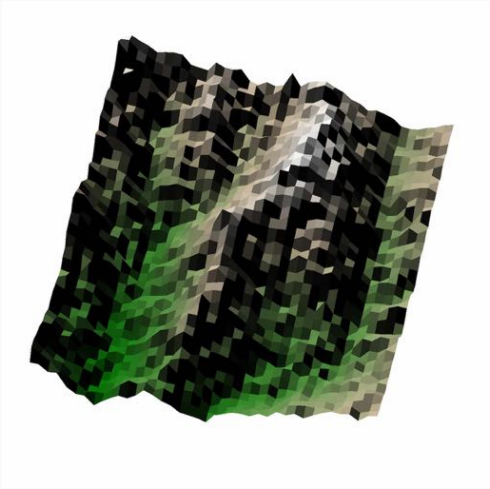

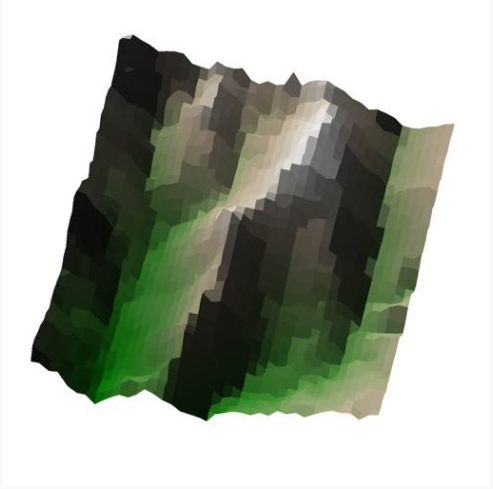

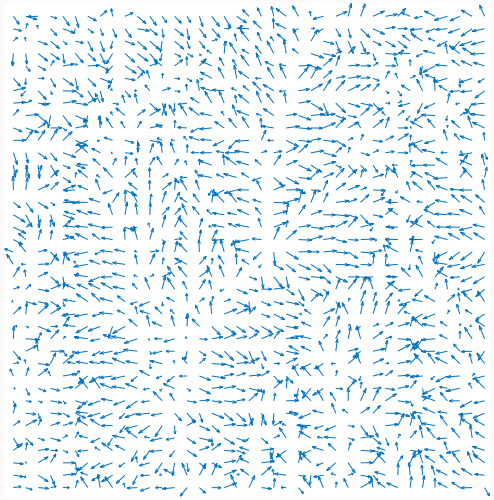

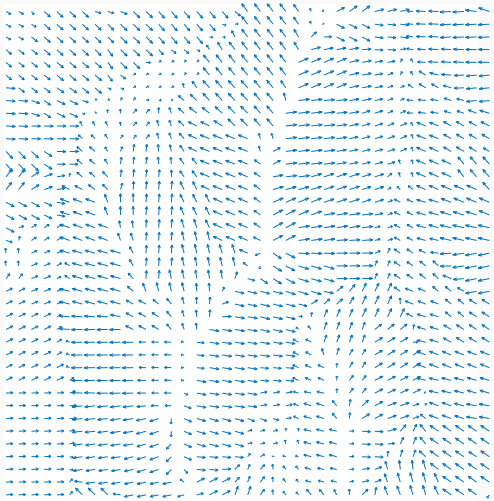

original data

[Geesch et al., 2009] via MFOPT
lellmann.net/software/mfopt

$p = 1$, $\lambda = 2$,
anisotrop.

Local image denoising

Light Detection and Ranging data (LiDaR), 40×40 pixel

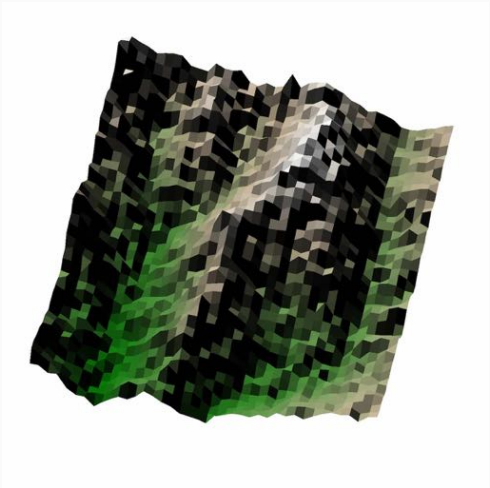

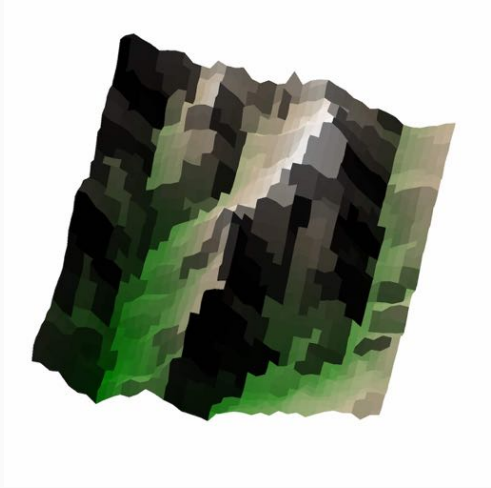

original data

[Geesch et al., 2009] via MFOPT
lellmann.net/software/mfopt

$p = 1$, $\lambda = 2$,
anisotrop.

$p = 0.1$, $\lambda = 1$,
anisotrop.

Nonlocal image denoising

- $\mathcal{M} = \mathbb{S}^1$, phase in $[-\pi, \pi)$, color: hue
- $V = \{1, \ldots, 256\} \times \{1, \ldots, 256\}$ pixel grid
- E from 12 most similar pixels w.r.t. 17×17 patch distances

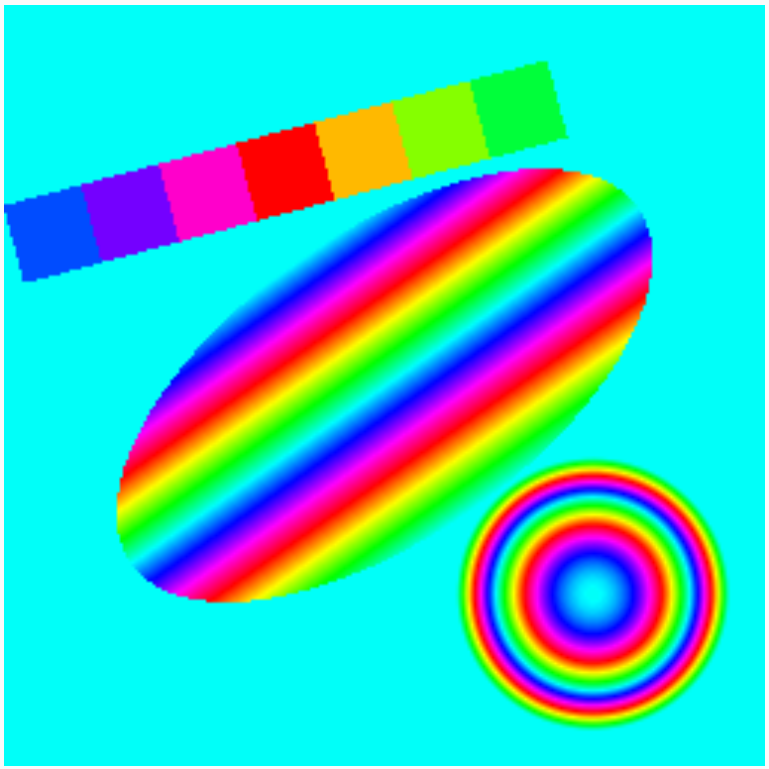

original.

Nonlocal image denoising

- $\mathcal{M} = \mathbb{S}^1$, phase in $[-\pi, \pi)$, color: hue
- $V = \{1, \ldots, 256\} \times \{1, \ldots, 256\}$ pixel grid
- E from 12 most similar pixels w.r.t. 17×17 patch distances

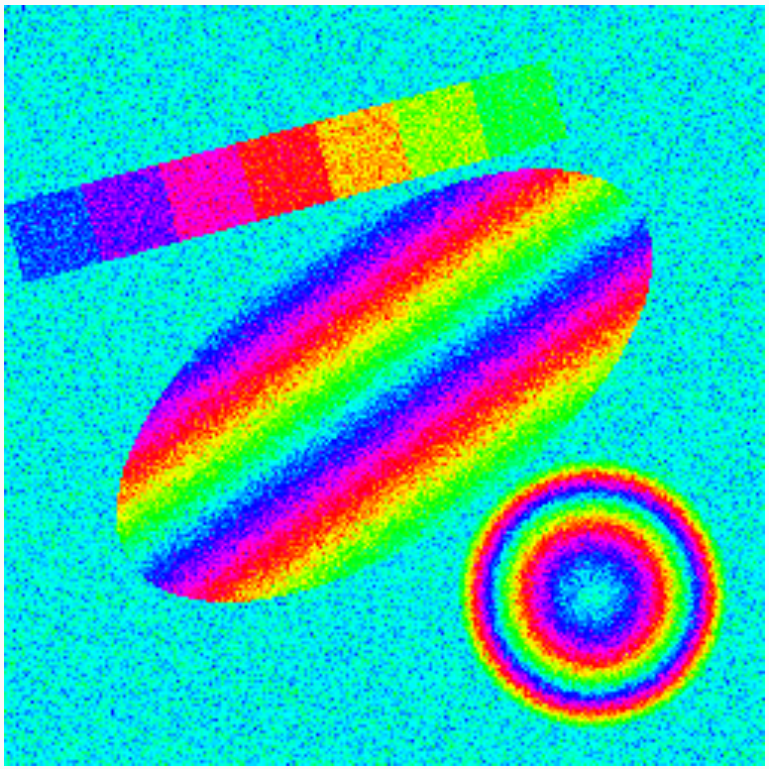

wrapped Gaussian, $\sigma = 0.3$.

Nonlocal image denoising

- $\mathcal{M} = \mathbb{S}^1$, phase in $[-\pi, \pi)$, color: hue
- $V = \{1, \dots, 256\} \times \{1, \dots, 256\}$ pixel grid
- E from 12 most similar pixels w.r.t. 17×17 patch distances

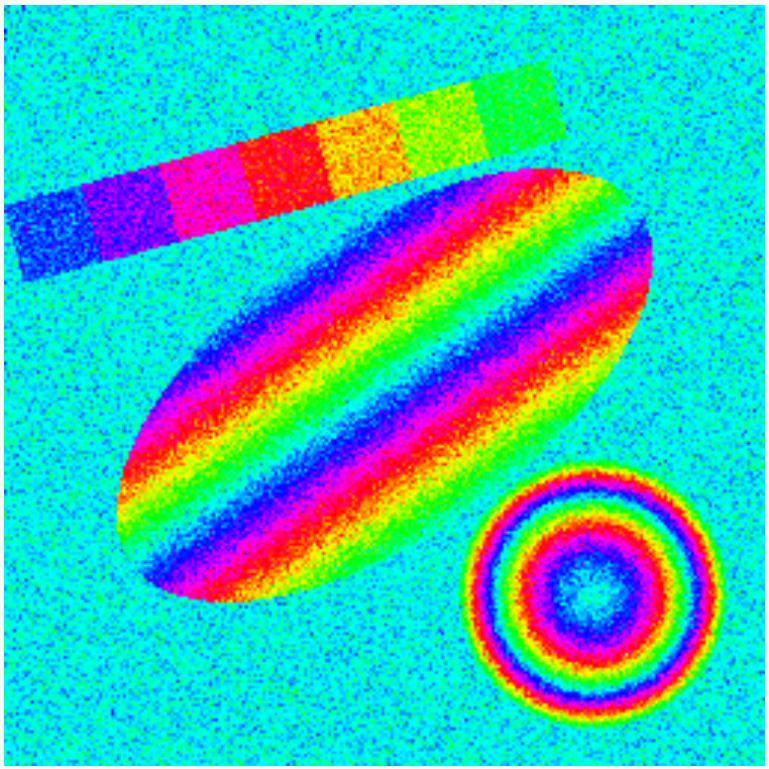

wrapped Gaussian, $\sigma = 0.3$.

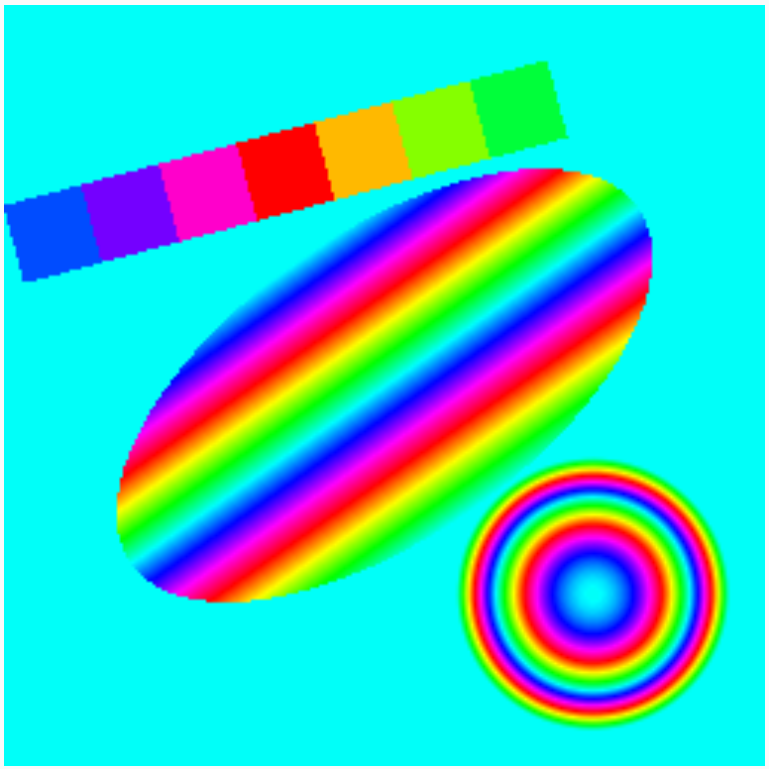

NL-MMSE. [Laus et al., 2017]

$\varepsilon = 2.50 \times 10^{-3}$

Nonlocal image denoising

- $\mathcal{M} = \mathbb{S}^1$, phase in $[-\pi, \pi)$, color: hue
- $V = \{1, \ldots, 256\} \times \{1, \ldots, 256\}$ pixel grid
- E from 12 most similar pixels w.r.t. 17×17 patch distances

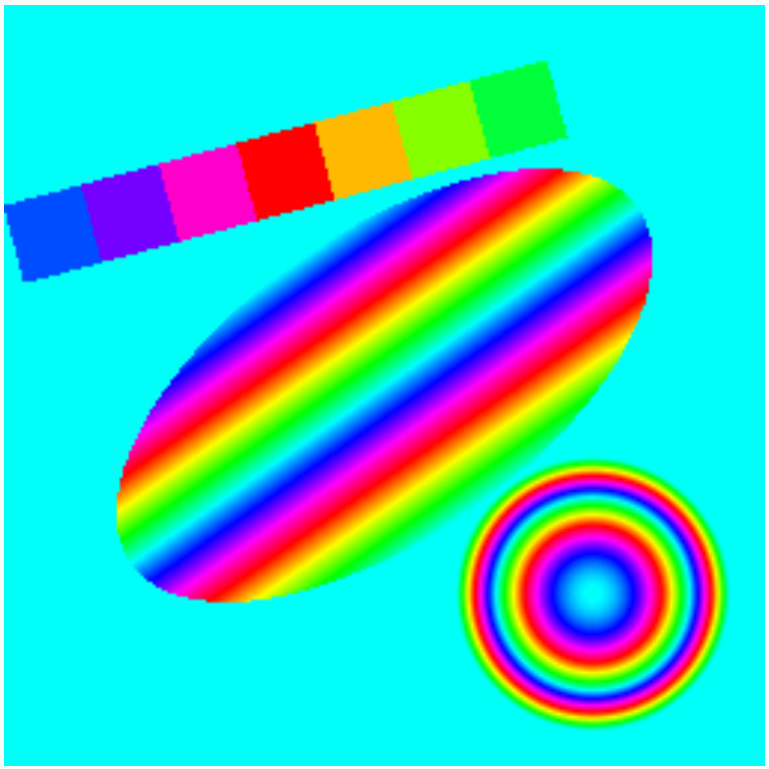

original.

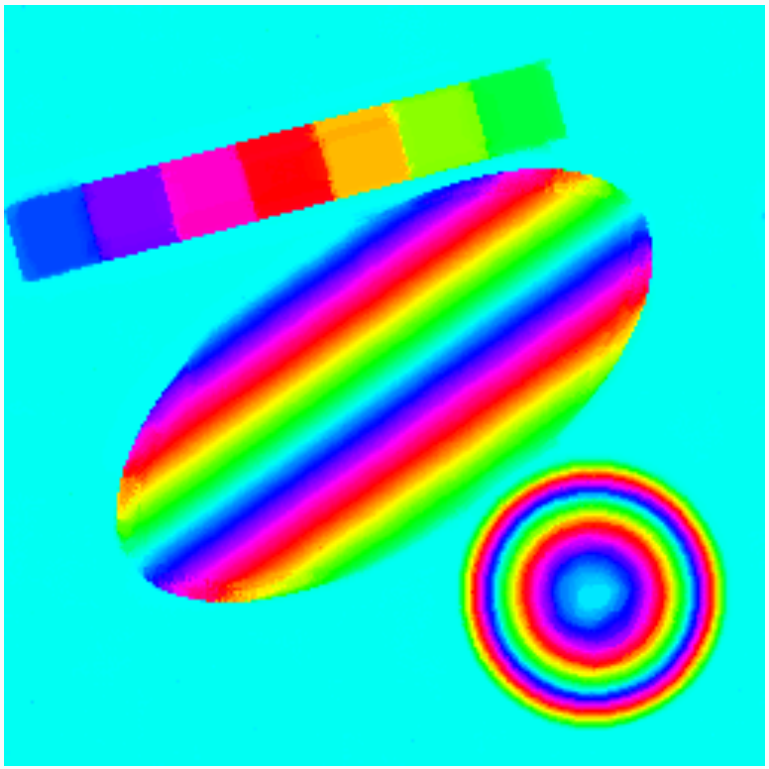

anisotropic, $p = 1$, $\lambda = 2^{-8}$, $\varepsilon = 2.67 \times 10^{-3}$.

Local denoising on a surface

- $\mathcal{M} = \mathcal{P}(3)$
- $V =$ point cloud: boundary of Camino dataset[1]
- local Neighborhood, $d_{\max} = 2$

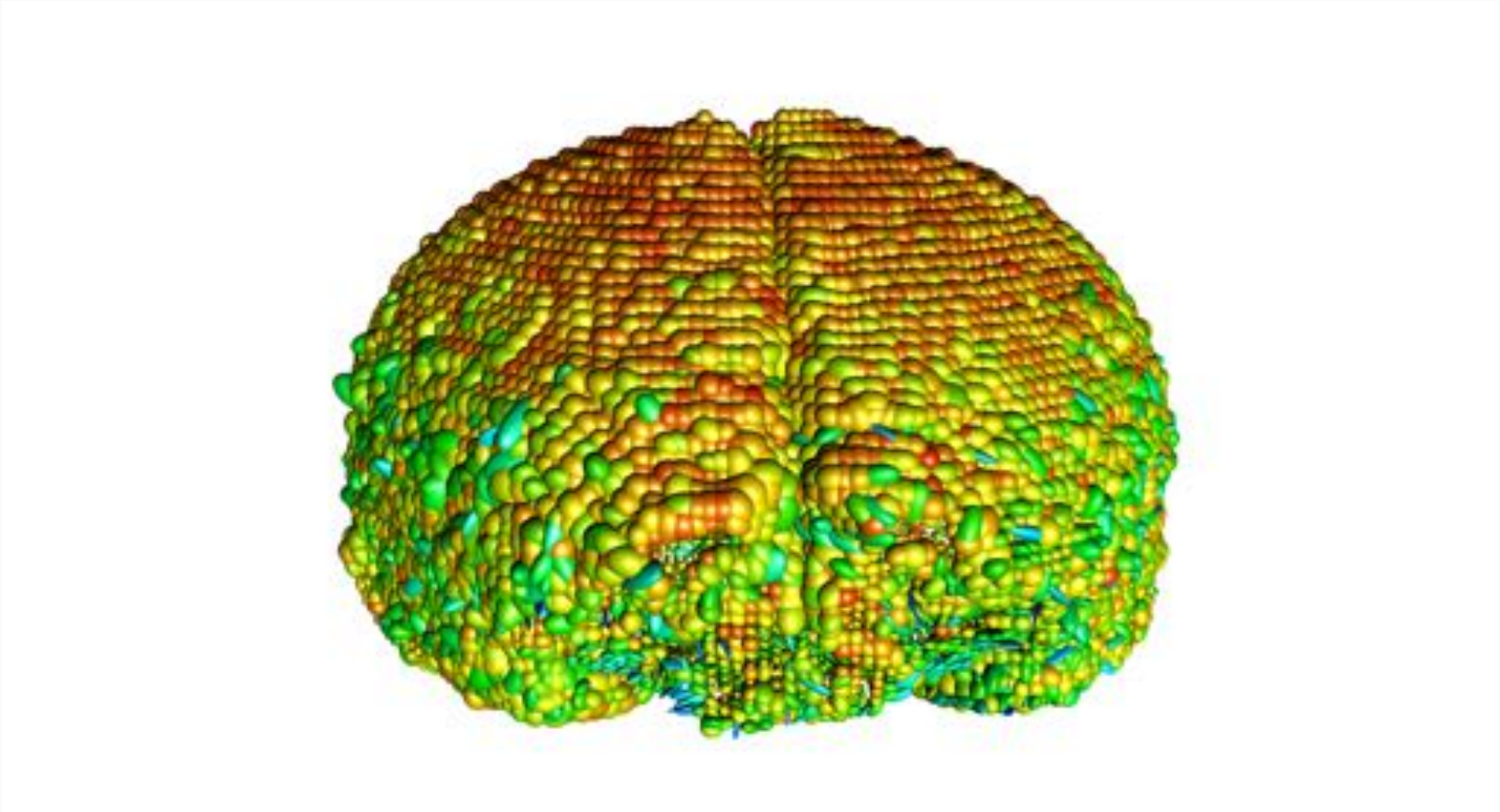

Original Data

Local denoising on a surface

- $\mathcal{M} = \mathcal{P}(3)$
- $V =$ point cloud: boundary of Camino dataset[1]
- local Neighborhood, $d_{\max} = 2$

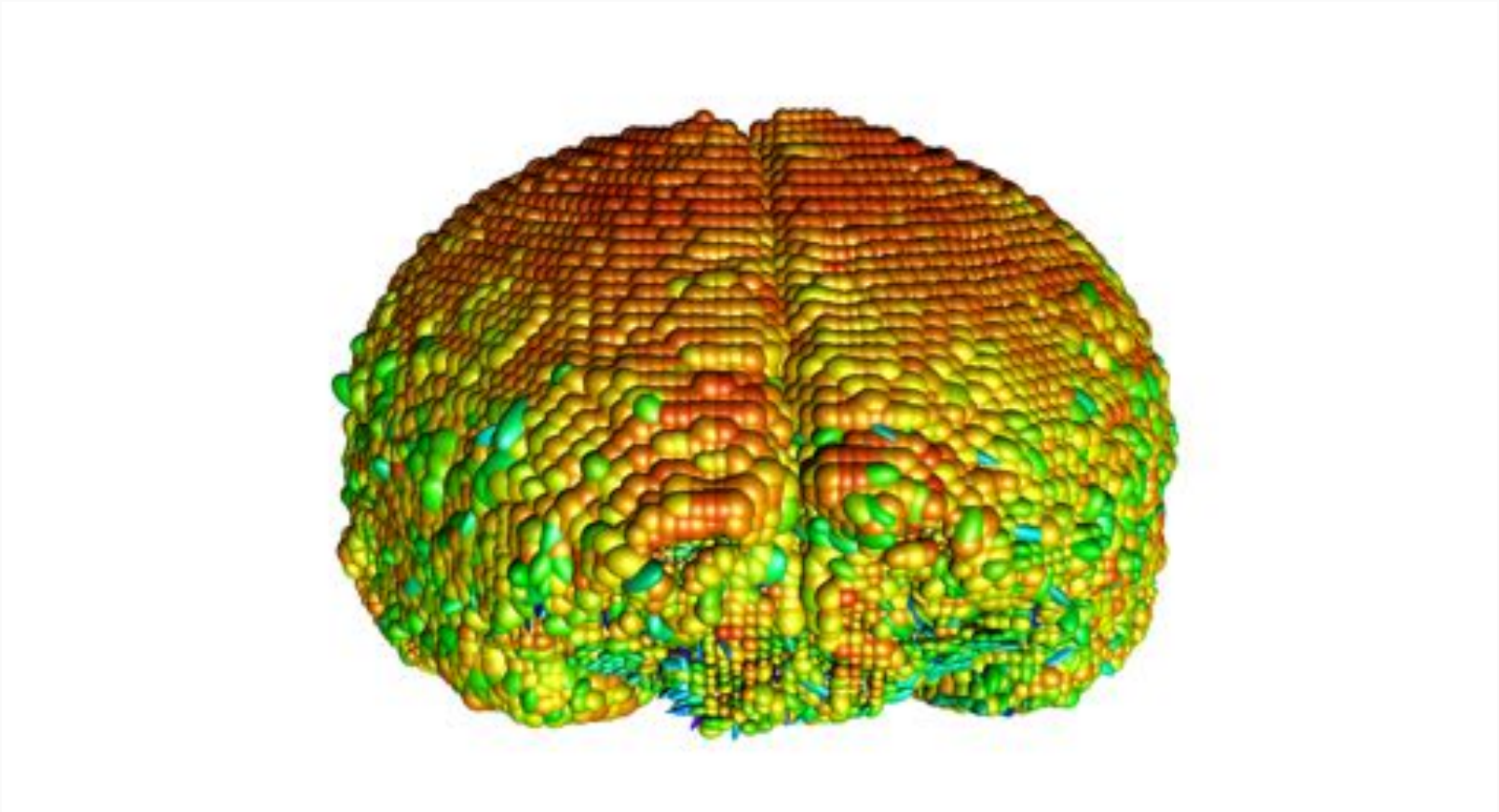

$\lambda = 50$, anisotropic 1-Laplace.

Summary

We have for manifold valued images $f\colon \mathcal{V} \to \mathcal{M}$

- a model for a first and second order TV-type functional $\mathcal{E}(u)$
- cyclic proximal point algorithm to minimize $\mathcal{E}(u)$
- proof of convergence
- Code available:

  http://www.mathematik.uni-kl.de/imagepro/members/bergmann/mvirt/

Furthermore manifold valued vertex functions $f\colon V \to \mathcal{M}$

- includes nonlocal methods and data on surfaces
- manifold valued graph p-Laplacian
- Code available soon.

Future work

- different couplings (infimal convolution)
- other algorithms
- applications to e.g.
  - DT-MRI
  - phase valued data
  - EBSD data
  - other manifolds?
- other image processing tasks
- continuous models

...and an implementation in Julia.

References


RB and D. Tenbrinck. A Graph Framework for manifold-valued Data. 2017. arXiv: 1702.05293.


RB, F. Laus, G. Steidl, and A. Weinmann. “Second order differences of cyclic data and applications in variational denoising”. In: SIAM J. Imaging Sci. 7 (4 2014), pp. 2916–2953.


M. Bačák, RB, G. Steidl, and A. Weinmann. “A second order non-smooth variational model for restoring manifold-valued images”. In: SIAM J. Sci. Comput. (2016). URL: http://arxiv.org/pdf/1506.02409v1.pdf.


RB, J. Persch, and G. Steidl. “A Parallel Douglas–Rachford Algorithm for Minimizing ROF-like Functionals on Images with Values in Symmetric Hadamard Manifolds”. In: SIAM J. Imag. Sci. 9.4 (2016), pp. 901–937.


RB, R. H. Chan, R. Hielscher, J. Persch, and G. Steidl. “Restoration of Manifold-Valued Images by Half-Quadratic Minimization”. In: Inv. Probl. Imag. 2.10 (2016), pp. 281–304.

Thank you for your attention.


RB and D. Tenbrinck. A Graph Framework for manifold-valued Data. 2017. arXiv: 1702.05293.


RB, F. Laus, G. Steidl, and A. Weinmann. “Second order differences of cyclic data and applications in variational denoising”. In: SIAM J. Imaging Sci. 7 (4 2014), pp. 2916–2953.


M. Bačák, RB, G. Steidl, and A. Weinmann. “A second order non-smooth variational model for restoring manifold-valued images”. In: SIAM J. Sci. Comput. (2016). URL: http://arxiv.org/pdf/1506.02409v1.pdf.


RB, J. Persch, and G. Steidl. “A Parallel Douglas–Rachford Algorithm for Minimizing ROF-like Functionals on Images with Values in Symmetric Hadamard Manifolds”. In: SIAM J. Imag. Sci. 9.4 (2016), pp. 901–937.


RB, R. H. Chan, R. Hielscher, J. Persch, and G. Steidl. “Restoration of Manifold-Valued Images by Half-Quadratic Minimization”. In: Inv. Probl. Imag. 2.10 (2016), pp. 281–304.